A PRIMER ON THE THERMODYNAMICS AND ECONOMICS OF STEAM-INJECTED GAS-TURBINE COGENERATION

Eric D. Larson
Robert H. Williams

PU/CEES Report No. 192

June, 1985

the center for energy and environmental studies

princeton university

ABSTRACT

Over the past decade, during which energy prices have been rising, cogeneration has become an increasingly attractive energy and money saving alternative to separate steam and electricity generation. Among cogeneration technologies, gas-turbine systems are attractive largely because of their lower capital cost and high thermodynamic efficiency when operating at full capacity. However, steam and electricity loads at typical industrial plants will vary daily and/or seasonally, contributing to lower capacity factors which, in turn, lead to less favorable economics for conventional gas-turbine systems.

Steam-injected gas-turbine cogeneration systems overcome the part-load problem by permitting excess process steam to be injected back into the turbine to raise the electrical generating efficiency and the output of electricity, any excess of which can be sold to the local grid at the prevailing avoided cost of electricity under provisions of PURPA. Based on the estimated cost of commercially available steam-injected systems, the rate of return from an investment in this cogeneration alternative at an industrial plant with a predictable daily load variation would be quite attractive in many parts of the US today, although not much greater than from a conventional gas-turbine system.

However, the risk incurred by a plant owner in investing in a steam-injected system is substantially lower than in most alternatives, since the flexibility to trade process-steam production for electricity generation virtually insures against any losses, e.g., due to unexpected long-term variations in the load or plant shutdowns. Use of the steam-injected cogeneration system instead of a conventional system will also result in significantly greater annual electricity production or considerable savings in fuel per unit of steam generated, making the technology attractive from society's perspective, as well as that of the user.

Steam-injected gas-turbines may eventually find applications in utility electricity base-load generation, since it appears that electrical generating efficiencies in excess of 50% can be obtained from turbines producing of the order of 100 MW of electricity at a fully-installed capital cost of around $500/kW.

TABLE OF CONTENTS

1. Introduction

Cogeneration, an energy and money saving alternative to the generation of electricity and steam for heating applications in separate facilities, was made considerably more attractive by the 1978 passage, and subsequent upholding by the Supreme Court, of the Public Utilities Regulatory Policies Act (PURPA), which requires electric utilities (i) to purchase power from qualifying cogenerators at a price that reflects the costs the utilities would avoid by not having to provide the electricity themselves and (ii) to provide back-up power at rates that do not discriminate against cogenerators.

A variety of cogeneration technologies are commercially available, including the gas turbine, the steam turbine, the gas turbine/steam turbine combined cycle, and the diesel engine. From a plant owner's perspective, the choice of one technology over another depends on the size of the plant's steam and electricity loads, the variability of the loads, the reliability of the system, fuel availability, and economics (e.g., expected return on investment).

Gas-turbine cogeneration is attractive because of its low installed capital costs compared to other cogeneration technologies (see Fig. 1), and its higher thermodynamic efficiency (second-law efficiency) in baseload applications (e.g., for meeting process heat loads in capital-intensive, energy-intensive industries characterized by relatively constant steam loads).

The recently introduced steam-injected gas-turbine extends the realm of applicability of gas turbines to cogeneration applications characterized by variable heating loads -- applications for which conventional gas

turbines are generally not well suited.

2. Technical Performance Measures of Cogeneration

Several technical performance indicators provide a basis for analyzing all cogeneration technologies.

2.1 First-Law Efficiency: The most universally understood measure of cogeneration performance is probably the overall first-law efficiency, defined as the ratio of the energy value of the useful heat and electricity produced to the heating value of the fuel consumed. By this measure, efficiencies for the separate production of electricity and steam (e.g., in a central station power plant and a stand-alone boiler) are in the 60 to 70% range. Steam-turbine cogeneration efficiencies are typically 80 to 90%; those for gas turbines and combined cycles, 70-80%; and for diesel cycles, 60-70% (see Table 1).

2.2 Fuel Chargeable To Power: Another measure is the amount of fuel chargeable to power (FCP) -- that portion of the total fuel consumption which would not have been needed to generate the same amount of process steam in a separate (stand-alone) boiler -- defined (in dimensionless units) as

$$FCP = (1 - S/BE)/E, \qquad (1)$$

where S and E are the fractions of the fuel converted to steam and electricity, respectively, and BE is an assumed efficiency for the stand-alone boiler. The FCP is commonly expressed in units of BTU/kWh, in which case Eqn. 1 becomes

$$FCP = 3413 * (1 - S/BE)/E. \qquad (1a)$$

At a central station generating plant, all of the fuel is used to produce electricity, typically yielding a FCP of about 2.93 kJ/kJ (10,000

BTU/kWh). For steam-turbine cogeneration, the FCP is typically less than half this value -- about 1.4 kJ/kJ (4700 BTU/kWh). For gas-turbine systems, it is of the order of 1.6 (5500), for combined cycles, 1.5 (5000), and for diesel engines, 2.0 (7000) (see Table 1).

Both the first-law efficiency and the FCP are useful energy performance indices in some evaluations, but they are somewhat misleading indicators of overall thermodynamic performance because they do not adequately account for the quality of energy embodied in the products of cogeneration. These indicators tend to favor cogeneration schemes that produce a relatively small amount of electricity per unit of process steam, such as steam-turbine systems, which typically convert only 10-15% of the fuel into electricity, but 65-75% into process steam (see Table 1). The higher electricity-to-steam ratios (ESR) of gas-turbines, combined cycles, and diesels mean they typically produce 4-8 times more electricity per unit of process steam than steam-turbines (see Table 1), and thus have the largest potential for generating electricity in excess of onsite needs for sale back to the grid.

2.3 Second-Law Efficiency: A better measure of overall thermodynamic performance, which takes into account the higher thermodynamic quality of electricity compared to steam, is the second law efficiency, defined as the ratio of the minimum available work required to produce steam plus electricity, B_{min}, to the actual available work used up in the process, B_{act} (American Institute of Physics, 1975). For a cogeneration system producing saturated process steam at a temperature, T, and pressure, P,

$$B_{min} = mv(p-p_o) + mc_p[(T-T_1) - T_o\ln(T/T_1)] + mh_{fg}[1-(T_o/T)] + E \qquad (2)$$

(Williams, 1978), where

m = the mass of saturated process steam at p

P_o = inlet pressure of the feedwater

T_1 = inlet temperature of the feedwater

v = specific volume of the feedwater

c_p = specific heat (at constant pressure) of the feedwater

h_{fg} = enthalpy of vaporization at pressure p

The available work in fossil fuels roughly equals the lower heating value (American Institute of Physics, 1975).

As shown in Table 1, second law efficiencies for separate steam and central station electricity generation are all about 0.35, while those for cogeneration range from 0.40-0.52, with the highest of these values corresponding to systems characterized by the highest ESRs -- gas-turbines, combined cycles, and diesels.

2.4 The Fuel Savings Rate: One additional measure, the fuel savings rate (FSR), also takes account of energy quality, but is somewhat less abstract than the second law efficiency. Defined as the amount of fuel saved in producing electricity (by cogeneration rather than central station generation) for each unit of process steam generated (Williams, 1978), the FSR is commonly expressed in dimensionless terms (e.g., kJ of fuel per kJ to steam) and is calculated from

$$FSR = (2.93 - FCP) * ESR. \quad (3)$$

As Table 1 indicates, the greatest fuel savings come from the cogeneration technologies that produce the largest amount of electricity per unit of process steam -- gas-turbines, combined cycles, and diesels.

3. Part-Load Performance of Gas-Turbine Cogeneration Systems

The attractive thermodynamics of gas-turbine cogeneration systems operating at full-load, as discussed in the preceding section, tends to degrade when running at part-load, as would be the case for a sizeable fraction of the year in many smaller scale industrial and commercial applications.

The part-load problem is illustrated in Fig. 2, which shows that the second law efficiency and the FSR drop precipitously in conventional gas-turbine systems when the process steam demand drops and the fuel input to the turbine is throttled (case C) (1). In addition, the FCP rises sharply and the electrical output drops off (see Fig. 3). Because of the poor part-load performance characteristics of a throttled turbine, the more commmon mode of operation is to bypass the steam generating system with the hot exhaust gases, allowing full electrical production to continue at the expense of an increasing FCP (see Fig. 3, case B). The second law efficiency falls off somewhat more slowly (see Fig. 2, case B), but the FSR drop is equally sharp. This poor part-load performance often leads to unfavorable economics. Thus, gas turbines have been restricted largely to applications where steam loads are relatively constant.

The recently-commercialized steam-injected gas-turbine, however, overcomes problems associated with part-load operation by providing (through only minor hardware modifications) for excess steam to be injected into the combustor, just after the compressor, of the turbine system. As a result of the greater mass and energy flows through the turbine, obtained without additional compressor work, net electricity production increases significantly, but the FCP increases only moderately (see Fig. 3, case A).

The second law efficiency remains essentially constant for all process-steam loads, while the FSR actually rises with increasing electrical output as the load drops (see Fig. 2).

When no process steam is required, the FCP at full steam-injection is significantly lower than that for most large central station power plants, even for the very small gas turbines focussed on in this paper (see Figs. 2 and 3)! This remarkable result has created interest in the use of full steam-injection for the generation of power only in central station power plants, for which it appears that at moderate sizes (~100 MW), FCPs of the order of 1.8 kJ/kJ (6200 BTU/kWh) are feasible (General Electric, 1984).

One of the keys to the viability of steam-injected gas-turbines in cogeneration applications is the availability of markets for excess electricity, which now exist as a result of the PURPA legislation. In addition, general apprehensions several years ago to investing in natural gas-fired equipment, arising from fears of significant increases in natural gas prices, have proved to be unfounded. The average price of natural gas paid by industry in the U.S. is currently projected to fall by about 12%, 1983-1995 (American Gas Association, 1985).

4. A Review of Conventional Gas-Turbine Cogeneration Thermodynamics

Conventional gas-turbine cogeneration systems embody an open Brayton cycle, with heat in the turbine exhaust used to produce steam in a heat-recovery steam generator (HRSG). The thermodynamic performance of the power and steam generating portions of such a system can be determined independently, as reviewed below (2).

4.1 The Simple Brayton Cycle: As indicated schematically in Fig. 4a, the standard open-cycle gas turbine system incorporates: a compression process

(state 1 to 2), requiring an input of work; a heat addition process (2 to 3); and an expansion process (3 - 4), by which work (or electricity) is produced. The quantities of greatest practical interest are net power output and electrical generating efficiency.

For stationary gas-turbine power plants, most analyses assume standard (ISO) ambient conditions -- a temperature of 15°C (59°F) at sea level pressure. On the T-S diagram, Fig. 4b, these correspond to P_1 and T_1. In addition, hardware constraints dictate: compressor pressure ratio (CPR = P_2/P_1); turbine inlet temperature (T_3); the mass flow of working fluid (ususally assumed to be air) through the compressor (MF_C); compressor adiabatic efficiency (EFF_C), defined as the work input required for isentropic compression divided by the actual work; turbine adiabatic efficiency (EFF_T), defined as the actual work output divided by the work output for isentropic expansion; and gearbox-generator efficiency (EFF_G), defined as the ratio of the electrical work output of the system divided by the net shaft work output.

The first step in the calculation is to determine the temperature of the compressor discharge. (Refer to Fig. 4 for states corresponding to the variables in the following analysis.) Assuming that the working fluid behaves as an ideal gas (an assumption used througout this paper), so that its enthalpy is only a function of temperature [h = h(T)], and that its specific heat, CP_C is constant (so that $\Delta h = CP_C * \Delta T$), the compressor outlet temperature is obtained from the isentropic compressor efficiency:

$$EFF_C = W_{Cs}/W_C = CP_C*(T_{2s}-T_1)/CP_C*(T_2-T_1) \quad (4)$$

or

$$T_2 = T_1 + (T_{2s} - T_1)/EFF_C \quad (5)$$

The assumption of constant specific heat is used in this equation, since

the difference between T_2 and T_{2s} is small, but its temperature dependence is taken account of in all other calculations (see Eqns. 31 and 32). For isentropic compression,

$$T_{2s} = T_1 * (P_2/P_1)^{[(k-1)/k]} = T_1 * CPR^{[(k-1)/k]} \quad (6)$$

where k is the ratio of the specific heat at constant pressure to that at constant volume.

The heat input required to the combustor (Q_{in}), assuming constant pressure combustion (3), and a constant specific heat, CP_{comb} is

$$Q_{in} = CP_{comb} * (T_3 - T_2) \quad (7)$$

In practice, heat addition adds mass -- the products of combustion -- to the working fluid and changes its specific heat. However, since typical turbine air-to-fuel ratios are in the neighborhood of 40:1, for a first-order analysis, the changes in mass flow and specific heat can be neglected (4).

The turbine exhaust temperature is calculated from the turbine isentropic efficiency,

$$EFF_T = W_T/W_{Ts} = CP_T*(T_4-T_3)/CP_T*(T_{4s}-T_3) \quad (8)$$

or

$$T_4 = T_3 - EFF_T*(T_3 - T_{4s}) \quad (9)$$

Defining the turbine pressure ratio as

$$TPR = P_4/P_3 \quad (10)$$

then

$$T_{4s} = T_3 * (TPR)^{[(k-1)/k]} \quad (11)$$

If pressure losses through the combustor and the pressure difference between the turbine outlet and ambient are neglected, TPR equals the inverse of CPR (3).

The net work output per unit mass flow is simply the sum of the

actual compressor and turbine work, expressions for which are given in Eqns. 4 and 8 (5):

$$W_{net} = W_T + W_C \tag{12}$$

The net shaft and electrical power outputs are

$$P_{sh} = MF_T * W_T + MF_C * W_C \tag{13}$$

$$P_{el} = P_{sh} * EFF_G \tag{14}$$

and the cycle shaft and electrical power production efficiencies are

$$EFF_{sh} = |W_{net}/Q_{in}| \tag{15}$$

$$EFF_{el} = EFF_{sh} * EFF_G \tag{16}$$

Using Eqns. 4-16, a number of pedagogically interesting calculations can be performed to understand the influences of different parameters on system performance. For example, Fig. 5 shows a simple-cycle performance map for a range of CPRs and turbine inlet temperatures (TIT). At a fixed TIT, it is observed that one value of CPR maximizes work output, and another maximizes efficiency, a result which can also be derived analytically (6).

4.2 The Heat-Recovery Steam Generator: The heat-recovergy steam generator (HRSG) usually consists of an economizer, in which the feedwater (part cold make-up and part condensate return) is heated to near its saturation temperature, and a boiler (or evaporator), in which the water is converted to saturated steam. If superheated steam is required, the saturated steam would then enter a superheater.

In some applications, a supplemental firing system -- a duct-burner -- is inserted between the turbine exit and the HRSG to provide the capability to increase the steam-generating capacity of the HRSG. Ample oxygen exists in the turbine exhaust to permit supplementary fuel to be completely

combusted in the duct burner. The high temperature of the turbine exhaust gases results in very high combustion efficiencies and correspondingly high steam-generating efficiencies (Wilson, 1978). The latter have been reported as high as 96% (lower heating value), compared to 80 to 90% for good stand-alone boilers (Kosla, Hamill, Strothers, 1983).

Energy Balances: For pedagogical purposes, the three sections of an HRSG can be considered as a single counterflow shell-and-tube heat exchanger, with the hot exhaust gases (from the turbine or the duct burner) passing in one direction on the shell side and water and/or steam traveling through tubes in the opposite direction. The temperature profiles in the HRSG as functions of the percent of heat transferred (or geometric distance in the simplified shell-and-tube conception) are shown in Fig. 6.

The gas-side temperature profile is essentially linear, since the heat tranferred per unit time from the gas, dq, along any section from point x to x+dx (see Fig. 6), can be expressed as

$$dq = MF_g * CP_g * (T_{x+dx} - T_x) \qquad (17)$$

where MF_g is the gas mass flow rate, CP_g is the specific heat of the gas per unit mass (which is assumed constant at its average value in the HRSG), and T_x and T_{x+dx} are the gas temperatures at points x and x+dx. The water/steam-side profiles will also be essentially linear, but with different slopes along each section of the HRSG (7). In the boiler, the temperature is a constant equal to the saturation temperature (T_{sat}) corresponding to the operating pressure of the HRSG.

In a HRSG with air and water as the working fluids, the closest point of approach between the gas and liquid temperatures at any point will be at the inlet to the boiler, the so-called pinch point (see Fig. 6), where the

temperature difference is defined as T_{pp} (8). From the gas-side inlet, (refer to Fig. 6), to the the pinch point, the total heat released per unit time by the gas is

$$Q_g = MF_g * CP_g * [T_1 - (T_{sat} + \Delta T_{pp})] \quad (18)$$

Typically 1-2% of this energy is lost by radiation or other means (Eriksen, Froemming, and Carroll, 1984), so that the actual heat absorbed by the liquid is

$$Q_{liq} = 0.98 * Q_g \quad (19)$$

The enthalpy change per unit mass of liquid between the superheater outlet and the pinch point is

$$\Delta h = h_1 - h_f \quad (20)$$

where h_1 is the enthalpy of the superheated steam exiting the HRSG and h_f is the enthalpy of saturated liquid at the HRSG pressure. (If no superheater is used, $\Delta h = h_{fg}$, the enthalpy of vaporization.)

Note that for any given system, there is an upper limit on the steam temperature at the superheater outlet (and hence on h_1), as determined by the temperature of the exhaust gas at that point. Based on practical considerations (9), the difference between these two temperatures (ΔT_{so}) is commonly in the range 15-30°C (30-50°F). Decreasing ΔT_{so} (i.e., increasing the superheat of the steam) has a relatively minor effect on the fraction of fuel input to a cogeneration system that is converted into steam, as shown in Fig. 7.

The mass flow rate of steam is calculated from Eqns. 19 and 20

$$MF_{st} = Q_{liq}/\Delta h \quad (21)$$

The stack-gas temperature (see Fig. 6) can be checked (to insure that

condensation will not occur) from an energy balance on the economizer, since the steam flow rate is now known, and an effective feedwater temperature, T_{fw} (a weighted average of the known make-up and condensate return temperatures) can be calculated

$$T_{stack} = T_{sat} + \Delta T_{pp} - \{MF_{st}*(h_f - h_{fw})*(1 + BD)/[(MF_g*CP_g)*0.98]\} \quad (22)$$

where h_{fw} is the enthalpy of saturated water at T_{fw} and BD is the continuous blow-down fraction -- an amount of saturated liquid at T_{sat} (expressed as a fraction of the steam flow) that is continuously added to and subsequently flushed from the system to prevent mineral buildup in the boiler. Blow-down fractions are typically about 0.05 (Eriksen, Froemming, and Carroll, 1984).

The Influence of the Pinch Point: The pinch point temperature difference plays two important roles in the design of a HRSG. As is evident from the Eqns. 18-22, for a fixed process steam quality and HRSG gas-side inlet temperature, ΔT_{pp} determines the steam flow that can be generated, or alternatively, the fraction of the original fuel that is converted to steam, which is a linearly decreasing function of ΔT_{pp} in a typical system (see Fig. 8) (10). The pinch point is also important in determining the HRSG heat-transfer surface area requirements, and consequently capital cost, which varies roughly as the inverse of the logarithm of ΔT_{pp} (see Fig. 8) (11).

The net influence of decreasing ΔT_{pp} is to increase the capital investment required per unit of steam generated. As seen in Fig. 8, this cost rises sharply in the neighborhood of 15-20°C (27-36°F) pinch points, a range typically used in current HRSG design practice (Cook, 1985) (12).

4.3 Textbook Variations on Simple-Cycle Cogeneration: The basic analyses

of the Brayton cycle and the HRSG presented above can be applied to systems incorporating regeneration, intercooling, or reheating, leading to cogeneration performance significantly different from that of the simple cycle, which is by far the most widely used gas-turbine cogeneration system today. Results of simple calculations (performed on a personal computer using spread-sheet software) are described in this section that illustrate some of these differences.

The Simple Cycle (Base Case): As a point of reference, the simple cycle calculation [incorporating the operating characteristics of the Detroit Diesel Allison 501-KB turbine (see Table 2)] yields an electrical output and fuel fraction converted to electricity of 3300 kW and 28%, respectively. Based on the available exhaust heat, the fuel fraction converted to steam and the steam production rate (saturated vapor at about 1.2 MPa (175 psia), assuming a pinch point temperature difference of 10°C, are 53% and 9510 kg/hr (20922 lb/hr), respectively.

Conventional Alternatives: Alternative cycle configurations usually considered for the gas turbine involve combinations of: heat exchange between the hot turbine exhaust gases and the relatively cooler compressor outlet gases through use of a regenerator to lower overall fuel requirements; multiple-stage compression with intercooling between each stage to decrease overall compressor work; and multiple-stage expansion with reheating between turbine stages to increase overall turbine work. These alternatives are shown schematically in Fig. 9, with results of several calculations shown in Fig. 10. One concludes that, compared to the simple cycle:

o regeneration alone does not alter the net electrical output, since

compressor and turbine work are unchanged; increases the fuel fraction converted to electricity, since some of the turbine exhaust heat is used to assist the combustor in heating the compressor discharge air; and decreases steam production and the fuel fraction converted to steam, since less of the turbine exhaust heat is being used in the HRSG (13).

- o intercooling alone increases net electrical output, since compressor work requirements are lower due to the lower average temperature during compression; does not affect steam production, since the turbine exhaust temperature is unchanged; and results in lower fuel fractions converted to both electricity and steam, because more fuel must be burned to heat the compressor discharge to the turbine inlet temperature (14).
- o reheating alone increases electrical output, since the average temperature in the turbine is higher; increases steam production, since the turbine exhaust temperature is higher; and raises the fuel fraction converted to steam, since the fraction converted to electricity falls (since the extra power is produced at a lower turbine pressure ratio) and the turbine exhaust temperature is higher (15).
- o regeneration combined with intercooling and/or reheating increases net electrical output, since compressor work requirements are lower and turbine work output is higher; increases the fuel fraction converted to electricity, decreases steam production, and decreases the fuel fraction converted to steam, all due to the dominating presence of the regenerator.

Figure 10 shows that gas-turbine systems can operate over a wide range of conditions, but hardware and/or economic constraints tend to dictate what is or is not done in practice. More elaborate systems could become more popular in the future, but it appears that the higher cost and greater complexity (and hence more difficult maintenance problems) associated with regeneration and multiple-stage compression and expansion cycles have acted thus far to limit the actual implementation of these often higher efficiency and/or output systems (Leibowitz, 1985).

5. The Thermodynamics of Steam-Injected Gas-Turbine Cogeneration

The curves for case A shown in Figs. 2 and 3 represent the performance of the steam-injected gas-turbine cogeneration system described in detail in this section (full steam demand in those figures corresponds to about 9000 kg/hr (19800 lb/hr) of saturated steam at 1.2 MPa (175 psia). As noted earlier, the FCP, second law efficiency, and the FSR all improve substantially over those for either of the two conventional options with steam-injected operation at part process-steam load.

Injecting water or steam into a gas turbine is not a particularly new idea, but only recently have steam-injection cogeneration systems been introduced. The steam-injected gas-turbine (STIG) cycle is described in textbooks [see, e.g., (Haywood, 1980) or (Diamant, 1970)], and in a number of other publications [see, e.g., (Maslennikov and Shterenberg, 1974), (Fraize and Kinney, 1979), (Davis and Fraize, 1979), (Brown and Cohn, 1981)]. The use of water (not steam) injection for short periods was commmon in the past for thrust augmentation in jet-aircraft engines, although this is now usually done with afterburners (Leibowitz, 1985). Water is injected into the combustors of many stationary gas turbines used

today to keep combustion temperatures low, thereby suppressing the formation of NO_x pollutants [see (Allen and Kovacik, 1984) and (Boyce, 1982)], to comply with pollutant emissions regulations in many states.

The enacting of PURPA has focussed attention on the steam-injection technology for cogeneration applications, primarily because of its flexible and highly efficient operation [(Leibowitz and Tabb, 1984), (Jones, Flynn, and Strother, 1982)]. Two US companies -- International Power Technology (IPT), Palo Alto, CA and Mechanical Technology, Inc. (MTI), Latham, NY -- now offer packaged STIG cogeneration systems based on the Allison 501-KH turbine (the 501-KB modified for steam injection). Dah Yu Cheng of IPT holds a patent (US Patent No. 4128994) which claims rights to the operation of any STIG cycle in the region of its peak electrical efficiency, which as subsequent calculations will illustrate, is defined uniquely for each STIG cycle.

5.1 A "Back-of-the-Envelope" Approach to the STIG Cycle: The basic operation of the STIG cycle involves generating steam with the turbine exhaust heat and injecting some or all of it back into the combustor (see Fig. 11). Thus, unlike the simple-cycle cogeneration calculations, the HRSG and turbine analyses are coupled. The peak electrical efficiency for a DDA-501 based system occurs when the HRSG generates a mass flow of steam for injection that is somewhat greater than 15% of the mass flow of air, as will be shown in detail later. This percentage can be used in a 4-step "back-of-the-envelope" calculation, providing a starting point for understanding how steam injection influences cycle performance.

Step 1: Reference Case: A simplified calculation using air as the working fluid yields a net electrical output (for an Allison 501-KH system)

of 3353 kW at an efficiency of 27% (16). This provides a reference for subsequent comparisons.

Step 2: "Free" Extra Mass: One result of steam injection is an increase in the mass flow through the turbine. To understand how this increase affects cycle performance, suppose first that the air flow through the turbine increases by 15%, and that the additional flow is supplied (in an unspecified manner) to the turbine inlet at the required temperature and pressure.

In most gas turbines, flow enters the turbine through a nozzle, the Mach number at the throat of which is typically unity, i.e., the flow is choked (Leibowitz, 1985). Thus, adding mass to the flow at the turbine inlet will induce a pressure rise at this point to the level which will permit the injected mass to flow through the nozzle throat (with Mach number still equal to one). This pressure rise is felt at the compressor outlet and results in a rise in the compressor pressure ratio, since (i) the compressor shaft rotation is constant [as determined by requirements of constant generator speed (1)] and (ii) the compressor, like nearly all turbo-machinery, is designed to move a constant volume of flow (Leibowitz, 1985).

As a result, the CPR for the Allison 501 turbine is increased from 9.3 to approximately (Jones, 1985)

$$CPR = 13.47*[(MF_T-MF_C)/MF_C] + 9.3 \qquad (23)$$

where MF_T and MF_C are the turbine and compressor mass flows (in kg/s), respectively. The incremental change in electrical output, P, and efficiency, Eff, with an incremental change in turbine mass flow (and hence CPR, as well), will be

$$d(P) = (dP/dMF_T)*dMF_T + (dP/dCPR)*dCPR \quad (24)$$

$$d(Eff) = (dEff/dMF_T)*dMF_T + (dEff/dCPR)*dCPR \quad (25)$$

For this case (17),

$$\Delta(P) = 554*\Delta MF_T + 22*\Delta CPR \quad (26)$$

$$\Delta(Eff) = 0.038*\Delta MF_T + 0.020*\Delta CPR \quad (27)$$

where ΔP is in kW when ΔMF_T is expressed in kg/s. Adding the increments predicted by these equations to the power and efficiency calculated in Step 1 yields an output of 4625 kW and an efficiency of 38%.

Step 3: Paying for the Extra Mass: The efficiency increase is large in step 2 because the extra mass was supplied "free" at the turbine inlet temperature and pressure. The next refinement in our calculation, therefore, is to account for the work and heat needed to raise the extra mass to the turbine inlet conditions.

Since we are ultimately interested in steam, we will neglect the work required to raise the mass to the turbine inlet pressure (pumping a liquid requires negligible work compared to compressing air). We will also assume that the extra mass enters the combustor as a vapor, which was a liquid before it was evaporated and heated to its injection temperature, T_{inj}, by heat recovered from the turbine exhaust. The total heat that must be supplied by burning fuel in the combustor in this case is, therefore,

$$Q_{in} = MF_C*CP_{comb}*(TIT - T_2) + (MF_T - MF_C)*CP_{inj}*(TIT - T_{inj})$$

where TIT is the turbine inlet temperature, T_2 is the compressor outlet temperature, and CP_{comb} and CP_{inj} are the specific heats of air and the injected fluid at their respective average temperatures in the combustor.

Equation 26 for the change in power output is applicable for this step, but Eqn. 25 becomes (18)

$$\Delta\,(\mathrm{Eff}) = 0.023*\Delta MF_T + 0.006*\Delta CPR \qquad (29)$$

where ΔMF_T is expressed in kg/s. Because of the additional heating that is required for the same output, the efficiency drops from 38 to 34%.

Step 4: The Specific Heat Effect: The last effect we need to account for is the difference in specific heats between our fluid in Steps 1-3 (air) and the actual injected fluid (water/steam). Because the specific heat of steam is roughly double that of air, we can expect an increase in turbine work output. We can also expect more heat to be recovered in the HRSG, since the gas-side temperature drop will be about the same as in the previous step. Despite the higher heat recovery, a higher heat input is expected in order to raise the steam temperature from T_{inj} to TIT (see Eqn. 28), since T_{inj} is limited by the turbine exhaust temperature (which does not change much from the previous step), not by the amount of energy recoverable in the HRSG.

The specific heat of the mixture passing through the turbine, CP_T (per unit mass of air flow) will be

$$CP_T = ST/A * CP_{st} + CP_{air} \qquad (30)$$

where ST/A is the mass ratio of injected steam to air. Figure 12 shows the variation with ST/A (at 1000 K) of the mixture specific heat parameters which enter into the turbine and HRSG calculations. For a ST/A = 0.15, CP_T is about 25% higher than CP_{air}.

Values of CP for steam (Marks, 1978) and air (Cain, 1985) (in units of kJ/kg-K) are given by

$$CP_{st} = [1.1 - 33.2*(T*1.8)^{-0.5} + 416.7*(T*1.8)^{-1}] * 4.178 \qquad (31)$$

$$CP_{air} = [0.24 + (2.415\times10^{-5}*(T*1.8)] * 4.178 \qquad (32)$$

where T (in Kelvin) is the average temperature at which the process occurs.

Three variables are changing from the reference case in this step. Thus the incremental changes in power output and efficiency are (19)

$$\Delta(P) = 689*\Delta MF_T + \Delta 86*\ CPR + 2027*\Delta CP_T \quad (33)$$

$$\Delta(Eff) = 0.021*\Delta MF_T + 0.008*\Delta CPR + 0.176*\Delta CP_T \quad (34)$$

where ΔP is in kW when ΔMF_T is in kg/s and ΔCP_T is in kJ/kg-K.

These equations, combined with the results in Step 1, predict a net electrical output of 5420 kW produced at an efficiency of 39%.

Summary: This "back-of-the-envelope" calculation illustrates two important facts about the steam-injected gas-turbine cycle.

- o Steps 2 and 3 demonstrate that since the compressor typically consumes 1/2-2/3 of the total turbine work output in a simple-cycle gas-turbine, any extra mass flow that can be provided to the turbine without requiring compression work will lead to an increase in both efficiency and net cycle work output. Steam is an ideal "extra" fluid, since it can be provided at high pressure with negligible compression work.
- o Step 4 demonstrates that the increase in specific heat of the fluid passing through the turbine is by far the most important effect. Since the results are so sensitive to changes in specific heat, accurate values (taking account of temperature dependence) need to be used throughout the entire cycle calculation.

5.2 Actual STIG Cycle Calculations: Accurately calculating actual STIG-cycle performance requires closer attention to detail than the simplified approach just described, but conceptually there are no differences, and indeed, the results of the "back-of-the-envelope" calculation turn out not

to be too far off. We will continue using the Allison-501 turbine in our analysis.

The procedure used here to calculate cycle efficiency and net power output as functions of ST/A requires initial specification of: compressor inlet temperature (T_1), turbine inlet temperature (TIT), steam-to-air ratio (ST/A), HRSG pressure, HRSG pinch-point temperature difference (ΔT_{pp}), temperature difference between the steam and the gas at the superheater outlet (ΔT_{so}), effective feedwater temperature (T_{fw}), and minimum HRSG exhaust temperature (T_{stack}).

The first step of the analysis is to calculate the compressor discharge temperature, as in the case of the simple Brayton cycle. Then, passing over the combustor for the moment, since TIT and ST/A are specified, the turbine calculation can be performed to give the turbine outlet temperature (TOT) and work output, also using the simple-cycle procedure, but with adjusted values for the specific heat parameters (20).

The saturation temperature corresponding to the HRSG pressure (which will be somewhat higher than the combustor pressure to permit injection) is used in the heat balance (Eqn. 21) on the boiler plus superheater (used to raise the steam temperature as high as possible) to find the enthalpy of the steam exiting the superheater. The steam injection temperature (T_{inj}) at this enthaply and HRSG pressure is obtained from the steam tables. If the calculated T_{inj} is higher than (TOT - ΔT_{so}), then T_{inj} is set equal to (TOT - ΔT_{so}).

The total heat addition to the cycle can now be calculated using Eqn. 28, which combined with the two work terms yields cycle efficiency.

Assuming TIT = 982°C (1800°F), ΔT_{pp} = 10°C (18°F), ΔT_{so} = 30°C (54°F),

and T_{stack} > 150°C (300°F), the calculated peak cycle efficiency occurs at a ST/A of about 0.17, as shown in Fig. 13. For ST/A up to this value, the constraint of ΔT_{so} determines the superheat temperature of the steam, as there is enough energy and "temperature" in the turbine exhaust to heat all of the steam to the maximum specified value (= TOT - ΔT_{so}). As ST/A continues to increase beyond this critical point, there is insufficient energy in the turbine exhaust to raise all of the steam to this temperature, so additional energy input to the combustor is required. Despite the additional work derived from the larger mass flow through the turbine, cycle efficiency begins to fall (21).

5.3 Part-Load STIG Operation: The analysis in the previous section applies to STIG cycles used in cogeneration applications, in that it shows that when process steam falls off, excess steam (22) injected back into the turbine will increase both the output of electricity and the efficiency at which it is generated, resulting in the attractive part-load performance characteristics seen earlier in Figs. 2 and 3 and also shown in Fig. 14.

The operating regime of a STIG cogeneration system, defined in terms of electrical output and steam generation, can be considerably expanded by the use of supplemental firing in a duct burner -- standard equipment on the systems offered by IPT and MTI -- as is evident in Fig. 15, reproduced from an IPT publication. IPT claims their system will operate anywhere within "Region A" -- electrical production from 3.5 to 6 MW and process steam production from 0 to about 13 MW (45 MBTU/hr) (International Power Technology, 1984).

5.4 STIG Hardware Considerations: STIG cycle thermodynamics are very attractive, but not all turbines are as easily adapted for STIG operation

as the Allison 501-KB, which is an aircraft-derivative turbine, and thus has a torque limit (6190 kW) considerably in excess of its design peak value (3500 kW). However, there are a number of aircraft-derivative turbines, such as the General Electric LM series, which appear to be well suited for steam-injected operation (General Electric, 1984).

The compressors used with steam-injected gas turbines must be designed to tolerate the backpressuring that occurs as a result of injection (see Eqn. 23). If the backpressuring is excessive, the compressor will stall -- a condition analogous to aircraft stall -- and the flow through the compressor will reverse. The stall margin, which determines the tolerable backpressure,

$$SM = 100*(CPR_{stall} - CPR_{design})/CPR_{stall} \qquad (35)$$

is 15-20% in most aircraft derivative turbines (Leibowitz, 1985), although some are substantially higher than this. For example, the unmodified Allison 501 compressor has a stall margin of over 45% (Leibowitz and Tabb, 1984). It is thus well-suited for STIG operation, since the CPR at peak efficiency with steam injection is only about 18% higher than the design CPR.

Two minor hardware modifications are required to operate the 501-KB in the STIG mode (Leibowitz and Tabb, 1984): (i) Steam manifolds must be added to the outside of the combustor case to permit steam to be injected at the outlet of the compressor (i.e., the combustor inlet); (ii) The power take-off (PTO) shaft, which connects the compressor shaft to the generator, must be strengthened, since in the standard turbine, it is designed to shear when subjected to a torque significantly higher than the design value. Related to this modification, the first-stage compressor

disc, which connects the first stage of compressor blades to the PTO shaft, must also be strengthened.

For injection alone, an Allison 501-KH-based STIG cycle consumes about 10600 liters/hr (2800 gal/hr) of water (at full injection) (International Power Technology, 1984). With the make-up and blow-down water, the STIG cycle consumes roughly 3 times as much water (operating at full injection) compared to a conventional gas-turbine cogeneration system. In addition, the water must be treated to remove minerals. The General Motors Company, which manufactures the Allison 501 turbine, recommends deionization of water for injection as steam into their 501-KH turbine to the same level of purification as water commonly injected for NO_x control (Cain, 1985).

5.5 Other Benefits of STIG: A number of benefits in addition to the strictly thermodynamic ones described earlier accompany STIG operation:

- With steam injection, turbine inlet temperatures can be kept lower than in a conventional turbine system while producing equivalent amounts of power. The IPT system operates at a peak TIT of 982°C (1800°F), while the Allison 501-KH has a rated peak of 1035°C (1895°F). Turbine engine life has been estimated to double with every 38°C (50°F) drop in TIT (Jones, Flynn, and Strother, 1982).
- In the DDA-501, since air bled from the compressor discharge is used to cool the first stage of the turbine (where the highest temperatures occur in the turbine), the injection of steam at the compressor outlet results in a coolant with both a lower temperature and higher heat capacity, resulting in more effective cooling of the first-stage turbine blades.
- The TIT can be kept relatively constant as the process load drops,

thereby avoiding some of the thermal stresses on turbine components that occur in conventional cycles at throttled operation.

- The injection of steam at the compressor discharge acts to suppress peak combustion temperatures, and hence the formation of NO_x pollutants. As noted earlier, water injection in existing gas-turbines is relatively common to meet NO_x regulations.
- The increased heat capacity of the gas-side fluid in the HRSG increases the rate of heat-transfer from the exhaust gas. Since the gas-side heat-transfer resistance dominates the overall heat transfer resistance from the gas to liquid [see (11)], a smaller heat exchanger surface area is required in the HRSG.

6. The Economics of STIG Cogeneration

The theoretical and practical thermodynamics of STIG-cycle cogeneration systems are quite attractive, but we have yet to address its cost. As of today, there are three installed STIG-cogeneration systems, all designed by IPT -- a single unit at San Jose State University, San Jose, California and dual units at a Sunkist Growers, Inc. processing plant in Ontario, CA (Koloseus, 1985). The installed capital costs for these systems have not been made public, because they probably overstate what these systems will cost once their use becomes more widespread. Probable total installed capital costs and incremental operating costs (beyond those for a stand-alone boiler plant), as estimated by IPT, are shown in Table 3.

To illustrate several approaches to analyzing the economics of STIG cycle performance, consider a hypothetical plant in California (where the 3 STIG systems have already been installed) currently operating a stand-alone

natural-gas fired boiler (83% efficient) to provide its in-plant steam requirements and purchasing electricity from the grid to meet electrical needs. To simplify the analysis, we will assume the plant's full steam demand to be 9090 kg/hr (20000 lb/hr) of 1.4 MPa (205 psig) saturated vapor (at the HRSG) and full electrical demand to be 3500 kW (corresponding to the maximum outputs of the IPT STIG-cycle oogeneration system with no steam injection and no supplemental firing). We will also assume a typical industrial plant load profile: full steam and electricity demand Monday-Friday from 7a.m. - 6p.m., and half demand at all other times (see Fig. 16a). Finally, we will neglect all subsidies and taxes in our analysis (investment tax credit, property tax, etc.)

6.1 Busbar Electricity Costs: The cost per kWh of producing electricity over the life of the hypothetical plant (busbar cost) can be determined as a function of the real interest rate, i, for alternative gas prices. The annualized (capital plus operating) lifecycle cost, over a plant life of N years, is

$$ALCC = (IC + TURBOH)*CRF(i,N) + FUEL + WATER + NTM + TS + INS \quad (36)$$

where

IC = present value of total installed ("overnight") capital costs ($5 million)

TURBOH = present value of all turbine overhaul costs over the life of the plant, which in 1985 dollars is

$$= 220{,}000 * \sum_{n=1}^{R} (1 + i)^{3n}$$ where R is the largest integer less than N/3.

CRF(i,N) = capital recovery factor

$$= 1/ \sum_{n=1}^{N} (1 + i)^{-n}$$

FUEL = annual incremental expenditures for fuel using the STIG system instead of the stand-alone boiler

$$= NGP * AV * \left(\sum_{n=1}^{T} FCP_n * HRS_n * kW_n\right)/10^6$$

where NGP = constant natural gas price ($/MBTU)$_{LHV}$

AV = plant availability (95% assumed)

T = total number of different power output levels (= 2)

FCP_n = fuel chargeable to power during STIG operation, assuming a stand-alone boiler efficiency of 83%, for each level of power output n [5422 BTU/kWH for n=1, 7576 for n=2 (23)]

HRS_n = hours/year of operation at power output level n (2860 for n=1, 5876 for n=2)

kW_n = power output at level n (3500 kW for n=1, 4750 for n=2)

WATER = annual costs for water injected as steam

= AV * GHR * HRS * DGAL

where GHR = thousand gallons of water used per hour during steam injection operation (= 1.4)

HRS = number of hours extra water is required (= 5876)

DGAL = $/1000 gallons for water (= 2.00)

NTM = non-turbine related maintenance above that required for the stand-alone boiler (= $60,000/yr)

TS = additional technical supervision (= $40,000/yr)

INS = insurance (= $37,500)

In California, natural gas averages $5.60/GJ ($5.91/MBTU) (based on the lower heating value (LHV); see Table 4). For a real interest rate of 10%, therefore, the cost in today's dollars of electricity over the life of the plant is about 5.2 cents/kWh (see Figure 17). By comparison, the average purchase price of electricity in California in 1983 was 6.4 cents/kWh, and in a number of other states average electricity prices were higher than California (see Table 5). At the current US average price for natural gas, the production of electricty by steam-injection at this

hypothetical plant appears competitive with the average purchase price of electricity from central station power plants.

6.2 The Internal Rate of Return: Most businesses make investments based on an expected internal rate of return, determined by setting the total initial investment required for the new plant equal to the total discounted operating-cost savings that result from replacing the existing facility and solving for the discount rate. From the previous section, the initial cost incurred to replace the existing stand-alone boiler is simply IC, the installed capital cost. To operate the STIG system requires some additional expenditures beyond what is required for the stand-alone boiler -- maintenance, fuel, water, supervision, and insurance, as described above. However, savings accrue from no longer having to purchase electricity and from being able to sell back any excess electricity at the prevailing avoided cost.

The calculation becomes slightly involved in our hypothetical California plant, since purchased electricity prices and avoided costs vary with the time of day and season of the year. For example, in the Pacific Gas & Electric (PG&E) territory in California, the purchased-electricity price structure includes peak, mid-peak, and off-peak rates, as does the avoided cost structure (see Table 6). In addition, there is a capacity charge applied to the peak power level reached each month by a purchaser of electricity and a capacity payment to a cogenerator if it can guarantee continuous delivery of firm power to the utility.

Taking account of all these factors, and using the PG&E rate structure, the internal rate of return has been calculated for five different scenarios, including one conventional gas-turbine system and four

alternative modes of steam-injected operation, as summarized in Table 7. The real (inflation-corrected) rates of return of 20-22% for all five cases are quite attractive. Somewhat surprisingly, however, from a plant owner's perspective, the STIG alternative does not appear to be much better an investment than the conventional system.

But focussing on the internal rate of return calculation obscures the fact that the plant owner incurs much less risk by investing in the STIG-cogeneration system, as an alternative to a simple-cycle gas turbine system. The steam load assumed in the above calculation (see Fig. 16a) varied predictably between two constant levels, a rather idealized situation. More typical load profiles are shown in Fig. 16b and 16c, but even these do do not account for unexpected shutdowns or other extreme changes in the load. With a seasonal load variation, such as that shown in Fig. 16c, rates of return are likely to be more attractive with the STIG system than with conventional operation, since the conventional system must be sized to meet the highest steam demand, which occurs for only a fraction of the year. Indeed, this is one reason the Sunkist fruit processing plant in California has installed a steam-injection system (Bendanillo, 1985).

In addition to the reduced financial risk to the cogenerator associated with the STIG option, the STIG system at the hypothetical plant, compared to the conventional alternative, is capable of annually producing up to 2/3 more electricity (with continuous full supplemental firing), or of saving nearly twice as much fuel per unit of process steam generated (with no supplemental firing, and additional electricity is production only when the process steam demand drops) (see Table 7). Thus the user's benefits from STIG are complemented by the societal benefits of a greater

power generating or a greater fuel savings potential than what is offered by the simple-cycle gas turbine.

6.3 The Short-Run Marginal Cost of Producing Electricity: If the short-run marginal cost (SRMC) of generation, i.e., the cost of fuel associated with the excess generation, is less than the prevailing avoided cost, it would be profitable for a STIG cogeneration plant to generate excess electricity when possible and sell it to the grid. Two situations can arise in which a STIG-cycle system could produce excess electricity.

Case A -- Without Supplemental Firing: If the plant does not require all of the steam that the STIG system can produce, steam not needed for process can be injected into the turbine to raise electrical output. Assuming the additional electricity generated is available for sale to the grid, the fuel charged to the incremental power production is

$$FCP_{incr} = (FCP_I * KWH_I - FCP_B * KWH_B)/(KWH_I - KWH_B) \quad (37)$$

where the subscript I designates quantitites under conditions when steam is injected and B designates quantities under conditions when excess turbine exhaust bypasses the HRSG to the stack. Under this condition, the incremental FCP is about 0.94 kJ/kJ (3200 BTU/kWh) (LHV) in the IPT STIG system (24) -- representing the additional fuel that is required to raise the temperature of the steam at injection up to the turbine inlet value. With natural gas selling at its average U.S. price in 1983, $4.89/GJ ($5.16/MBTU) (LHV), the avoided cost only needs to be about 1.6 cents/kWh to make it economical to inject excess steam and produce additional electricity for sale to the grid (see Fig. 18).

Case B -- With Supplemental Firing: From the results of Case A, when no supplemental firing is used, it makes sense to always inject excess

steam and sell the extra electricity to the grid. This is taken as the reference point for the second case, in which the SRMC will determine whether to supplemental fire the system to generate even more electricity for sale to the grid, while continuing to meet the process-steam demand. Under this condition

$$FCP_{incr} = (FCP_S*KWH_S - FCP_I*KWH_I)/(KWH_S - KWH_I) \quad (38)$$

where the subscript S designates quantities when supplemental firing is used, the incremental FCP is about 3.96 kJ/kJ (13,500 BTU/kWh) (LHV) (25). From the plant owner's perspective, therefore, supplemental firing for the sole purpose of selling additional electricity to the grid will only make sense if avoided costs are considerably higher than in Case A, as shown in Fig. 18.

However, the incremental FCP in Case B is essentially the same as the FCP for gas-tubines used by utilities to meet peak loads (Electric Power Research Institute, 1979). Thus, a steam-injected cogeneration system with supplemental firing capability could be "free" peaking capacity to a utility, provided an agreement is reached with the cogenerator to make the capacity available on demand.

7. The Future of STIG

Larger steam injected gas turbine systems, operating at higher pressure ratios and turbine inlet temperatures, are under active development. Based on modelling and some preliminary tests, the General Electric Company (GE) indicates that with only minor modifications, the electrical output of their LM-5000 turbine could be raised from 33 MW in the conventional mode to 50 MW in the steam-injection mode, while the

efficiency in generating electricity alone would rise from 37% (LHV) to 44% (LHV) (General Electric, 1984). With another 2-3 years of developmental work, GE indicates that 108 MW could be produced at an efficiency of 55% by a system using intercooling with steam injection (26). A back-of-the-envelope calculation indicates that this level of performance is thermodynamically attainable.

The Simpson Paper Company near Anderson in Northern California currently operates an LM-5000 turbine in a conventional cogeneration configuration. Before the end of the year, they will be making the minor modifications necessary to inject steam, and thus produce electricity at up to 44% efficiency (LHV) (Price, 1985). An agreement to sell electricity to the PG&E Utility has already been reached.

Steam-injected gas-turbines operating on natural gas may come to compete successfully with large coal-fired power plants for utility base-load generating capacity in many regions of the country. The favorable economics for central station STIG plants arise from very low capital costs [installed capital costs (in 1984$) of around $500/kW (General Electric, 1984), compared to $1200-1500/kW for large coal-fired facilities (Bechtel Power Corporation, 1981)], and relatively low fuel costs [because of efficiencies as high as 55% and expectations that natural gas prices will remain essentially constant for the next 10-15 years in many regions of the US (American Gas Association, 1985)]. Finally, much shorter construction lead times and the capability to make incremental additions (~100 MW) to the generating base with STIG systems would help utilities avoid the inherent risk-taking involved in embarking on expensive 7-10 year construction projects, which may eventually not be needed due to slower-

than-expected growth in demand for electricity during the construction period.

Utilities might also utilize STIG cogeneration systems as "electrical peaking systems." In the non-supplementary-fired mode, these systems could provide steam for process needs and base-load electricity, while supplementary firing could be used to provide extra steam for injection to meet peak electrical demands.

PG&E is pursuing still another STIG application. Under a PG&E plan being actively discussed (Price, 1985), aging boilers which produce steam for heating about 100 commercial buildings in San Francisco will be replaced by a single STIG system based on the LM-5000 turbine, thereby allowing PG&E to increase its base-load electricity production during the warmer months of the year when steam demands drop and electricity demands rise.

NOTES

1. To reduce process-steam production in conventional gas-turbine cogeneration systems, the fuel flow to the turbine can be throttled, resulting in lower turbine inlet and outlet temperatures, or the hot turbine exhaust can be bypassed around the heat recovery system. These are the only two alternatives in nearly all gas-turbine systems used to generate electricity, since most incorporate only a single shaft for the compressor, turbine, and generator. Since the generator speed must be maintained constant (and turbo-machinery is designed to move a constant volume of air at a fixed rpm), the mass flow through the system cannot be throttled.

2. Standard undergraduate thermodynamics textbooks describe gas-turbine cycle analysis. See, e.g., (Wark, 1977) or (Sonntag and Van Wylen, 1982). The analysis of heat recovery steam generators can be found in some texts [see, e.g., (Fraas, 1982)], and an excellent review can be found in (Eriksen, Froemming, and Carroll, 1984).

3. The actual pressure loss across the combustor is of the order of 5% of P_2. The actual turbine outlet pressure is of the order of 5% above P_1. These corrections have been made in the most detailed calculations in the paper.

4. For an air fuel ratio of 40:1, the mass flow through the turbine will be about 2% greater than that through the compressor, as a result of the addition of the combustion products, and the average value of the specific heat in the turbine will increase slightly. The additional mass flow has been taken into account in the most detailed calculations in this paper, but changes in specific heat due to addition of the combustion gases have been neglected.

5. The sign convention implicit in Eqns. 4, 7, 8, and 12 is that work or heat input to the cycle is positive, and that from the system is negative. This sign convention requires the absolute value symbols in Eqn. 15.

6. The CPR which will maximize work output from a simple Brayton cycle can be determined analytically if one assumes that the turbine pressure ratio is the inverse of the compressor pressure ratio (TPR = 1/CPR) and that specific heats are constant. The expression for net work output, obtained from Eqns. 4-6 and 8-11,

$$W_{net} = CP_C*T_1*(CPR^{[(k-1)/k]} - 1)/EFF_C + CP_C*T_3*EFF_T*(CPR^{-[(k-1)/k]} - 1) \qquad (N.1)$$

is differentiated with respect to CPR, set equal to zero, and solved for CPR. The resulting expression gives the value of CPR which maximizes work output

$$CPR_{maxw} = (EFF_T*EFF_C*TIT/T_1)^{[k/(2*(k-1))]} \qquad (N.2)$$

A similar exercise for determining the value of CPR that maximizes efficiency is left to the reader.

7. The water/steam-side temperature profile in an HRSG is essentially linear in each section due to the fact that the liquid-side enthalpy along any point in the economizer (containing a slightly compressed liquid) or the superheater (containing steam at low pressure and moderate temperature, and therefore well approximated as an ideal gas) is only a function of temperature, assuming specific heats are constant. Thus Eqn. 17 applies with 'water/steam' substituted for 'gas' in either the economizer or the superheater. In the boiler, of course, the temperature is a constant equal to the saturation temperature at the HRSG pressure.

8. The location of the pinch point can be understood from heat balances written for any section of the superheater (a similar analysis applies to the boiler and economizer). The heat transferred from the gas and to the steam between any points a and b are

$$Q_g = MF_g * CP_g * (T_{g,a} - T_{g,b}) \qquad (N.3)$$

$$Q_{st} = MF_{st} * CP_{st} * (T_{s,a} - T_{s,b}) \qquad (N.4)$$

Since these must be equal, and the product of mass flow and specific heat on the steam side (in any section of the HRSG) is usually in the range of 1/4 to 2/3 that on the gas side, the gas side temperature drop will always be less than the steam-side gain. Thus, the closest approach between the gas and water/steam temperatures inside the HRSG will be at the inlet of the boiler.

9. The temperature difference between the turbine exhaust and the superheater outlet, ΔT_{so}, is limited by two main considerations: (i) As ΔT_{so} decreases, heat transfer surface area, and consequently cost, increases, and (ii) ΔT_{so} must be designed to insure that the pinch point temperature difference, ΔT_{pp}, will never be negative.

10. The fuel fraction converted to steam, shown in Fig. 8, is obtained from a calculation which assumes a HRSG inlet (turbine exhaust) temperature of 477°C (891°F) and the production of saturated process steam at 177°C (351°F) [corresponding to a pressure of about 1.0 MPa (150 psig)]. From Eqn. 21, neglecting the 2% radiation losses (see Eqn. 19) and assuming a gas-side specific heat of 1 kJ/kg-K (0.24 BTU/lb-R), the mass flow of steam (kg/sec) for a turbine exhaust flow of 15 kg/s (33 lb/s) (about that in a system using a Detroit Diesel Allison 501-KB turbine -- see Table 2) is

$$MF_{st} = 2.22 - (\Delta T_{pp}/135) \qquad (N.5)$$

where ΔT_{pp} is the pinch point temperature difference. The estimated rate of heat input to a Detroit Diesel Allison 501-KB cogeneration system is used as the denominator to calculate the fuel fraction converted to steam (see Section 4.1 in the text).

11. The results for HRSG cost, shown in Fig. 8, are obtained from a

calculation which assumes the boiler and economizer to be one single-pass shell-and-tube heat exchanger, with a gas inlet temperature of 477°C (891°F), a boiler temperature (T_{sat}) of 177°C (351°F), a gas flow rate of 15 kg/s (33 lb/s), an effective feedwater (economizer inlet) temperature (T_{fw}) of 67°C (153°F), and gas and economizer specific heats of 1 and 4.2 kJ/kg-K (0.24 and 1.0 BTU/lb-R), respectively. The heat transfer surface area, S, required in the boiler and economizer are calculated separately from an equation of the form

$$S = q/U/\Delta T_{lmtd} \qquad (N.6)$$

where q is the heat transfer rate, U is the overall heat transfer coefficient, and T_{lmtd} is the so-called log-mean-temperature-difference.

The heat transfer rates in the boiler (Q_b) and economizer (Q_e) are

$$Q_b = MF_{st} * \Delta h_{fg} \qquad (N.7)$$

$$Q_e = MF_{st} * CP_e * (T_{sat} - T_{fw}) \qquad (N.8)$$

where Δh_{fg} is the enthalphy of vaporization at the boiler temperature, MF_{st} is the (unknown) steam flow rate, and CP_e is the specific heat of water in the economizer.

The overall heat transfer coefficient, U, is composed of three thermal conductances in series

$$U = 1/(1/U_w + 1/U_t + 1/U_g) \qquad (N.9)$$

where, U_w is a water/steam-side convection term; U_t is a heat-exchanger tube conduction term, and U_g is a gas-side convection term. The gas-side term limits the heat transfer, since it is of the order of 0.04 kW/m^2-°C (7 BTU/hr-ft^2-°F), while typical values for U_w are of the order of 11 kW/m^2-°C (2000 BTU/hr-ft^2-°F) in the boiler, 0.1 times this value in the economizer, and (for 0.3 cm (0.12 inch) thick steel tubing) the value of U_t is of the order of 11 kW/m^2-°C (2000 BTU/hr-ft^2-°F). To a good first approximation, therefore, U can be taken to be equal to U_g. A value of 0.04 kW/m^2-°C (7 BTU/hr-ft^2-°F) is used in this analysis (Cook, 1985).

The definition of the log-mean-temperature-difference, ΔT_{lmtd}, can be found in standard heat transfer textbooks [see, e.g., (Chapman, 1974)]. For this analysis, ΔT_{lmtd} in the boiler and in the economizer are,

$$\Delta T_{lmtd,b} = \{(TOT - T_{sat}) - (\Delta Tpp)\}/\ln\{(TOT - T_{sat})/(\Delta T_{pp})\} \qquad (N.10)$$

$$\Delta T_{lmtd,e} = \{(\Delta T_{pp}) - (T_{stack} - T_{fw})\}/\ln\{(\Delta T_{pp})/(T_{stack} - T_{fw})\} \qquad (N.11)$$

where TOT, the turbine outlet temperature, is assumed to be 477°C (891°F); T_{sat}, the HRSG saturation temperature, is taken to be 177°C (351°F); ΔT_{pp} is the pinch point temperature difference; T_{stack} is the gas-side outlet temperature (a weak function of ΔT_{pp} which can be determined from Eqn. N.8), and T_{fw}, the economizer feedwater temperature, is assumed to be 67°C (153°F).

To determine the surface areas of the boiler, S_b, and economizer, S_e, the rates of heat transfer to the boiler and economizer (Eqns. N.7 and N.8)

are set equal to the corresponding rates from the gas

$$Q_{g,b} = MF_g * CP_g * (TOT - T_{sat} - \Delta T_{pp}) \quad (N.12)$$

$$Q_{g,e} = MF_g * CP_g * (T_{sat} + \Delta T_{pp} - T_{stack}) \quad (N.13)$$

Equating Eqns. N.7 and N.12 yields an expression for MF_{st} in terms of ΔT_{pp} [see (10)], which is then substituted into Eqn. N.6 (written for the boiler) to get the boiler surface area as a function of ΔT_{pp}. A similar procedure using Eqns. N.8, N.13, and N.6 yields the surface area of the economizer as a function of ΔT_{pp}.

The total cost of the HRSG in 1985 dollars is then

$$\$HRSG = 3*(S/0.0929) + 60{,}000*[1 - \exp(-S/0.0929/3600)] \quad (N.14)$$

where S is the total heat transfer surface area in m^2 -- in this case $S = S_b + S_e$. This equation was developed by curve fitting HRSG prices for a standard line of [4 MPa (600 psig) design pressure] heat recovery units made by the Deltak Corporation (Cook, 1985). The equation is accurate to within about $\pm$20% for units with 200-9000 m^2 (2000-100000 ft^2) of surface, which covers most units used with gas turbines producing 0.5-100 MW of electricity.

The total cost of a complete HRSG unit, including a duct burner to provide supplementary firing capability (which, in turn, requires upgrading of the boiler) and auxiliaries, is estimated to be about double \$HRSG (Lovell, 1985) and is shown in Fig. 8.

12. The steam cost calculation assumes a plant life of 20 years, a 10% real interest rate, a steam flow given by Eqn. N.5, and a capacity factor of 90%.

13. In addition to assumptions used in the simple-cycle analysis, a value for the regenerator effectiveness, EFF_R, must be assumed in order complete regenerative-cycle calculations. The EFF_R is defined as the actual enthalpy change through the cold side (state 4 to 5 in Figure 9) divided by the maximum possible enthalpy change (state 4 to 9). Assuming constant specific heats,

$$EFF_R = (T_5 - T_4)/(T_9 - T_4) \quad (N.15)$$

An effectiveness of 0.8 is used in the calculation. With the compressor outlet and turbine exhaust temperatures known, Eqn. N.15 allows T_5 to be determined, based on which the required external heat input to the cycle can be calculated.

14. The intercooing calculation was done so as to minimize total compressor work. If it is assumed that $T_3 = T_1$ and $T_4 = T_2$ (see Figure 9) and that specific heats are constant, it can be shown that the pressure ratio across each stage of a two-stage compressor that minimizes overall work is the square root of the overall pressure ratio [see, e.g., (Wark, 1977)].

15. The reheat-cycle calculation was done so as to maximize total turbine

output from a 2-stage turbine. Assuming $T_7 = T_5$ and $T_8 = T_6$ (see Figure 9), the value of the pressure drop across each stage which maximizes total turbine work is the square root of the total pressure drop [see, e.g., (Wark, 1977)].

16. In step 1 of the "back-of-the-envelope" calculation, net power output, P, and cycle efficiency, Eff, are determined from the following expressions, derived from section 4.1 in the text

$$P = [MF_C*CP_C*T_1*(CPR^{a_C} - 1)/EFF_C + MF_T*CP_T*TIT*EFF_T*(CPR^{-a_T} - 1)]*EFF_g \quad (N.16)$$

$$Eff = P/\{MF_C*CP_{comb}*(TIT-T_1-T_1*(CPR^{a_C} - 1)/EFF_C)\} \quad (N.17)$$

in which subscripts C and T designate compressor- and turbine-related quantities, respectively. MF is mass flow, CP is specific heat at constant pressure, CPR is the compressor pressure ratio, EFF are efficiencies, 'a' is R/CP (R = gas constant for particular fluid), T_1 is the compressor inlet temperature, TIT is the turbine inlet temperature, and the subscripts 'comb' and 'g' refer to the combustor and gearbox-generator.

Assumptions used in these equations include: $MF_C = MF_T = 14.7$ kg/s (32.3 lb/s), CPR = 9.3, $T_1 = 15^oC$ (59^oF), $EFF_C = 0.833$, and $CP_C = 1.1$ kJ/kg-K (0.26 BTU/lb-R), $CP_T = CP_{comb} = 1.2$ kJ/kg-K (0.29 BTU/lb-R), TIT = 982^oC (1800^oF), $EFF_T = 0.897$, $EFF_g = 0.93$, and R = 0.287 kJ/kg-K (0.069 BTU/lb-R).

17. To determine the change in net power output and cycle efficiency when additional flow is injected into the turbine, Eqns. N.16 and N.17 can be differentiated to yield the coefficients of Eqns. 24 and 25, e.g.,

$$dP/dMF_T = CP_T*TIT*EFF_T*(CPR^{-a_T} - 1) \quad (N.18)$$

$$dP/dCPR = (\partial P/\partial M_T)*(\partial MF_T/\partial CPR) = \quad (N.19)$$

$$(13.47/MF_C)*\{a_C*MF_C*CP_C*T_1*CPR^{(a_C-1)}/EFF_C - a_T*CP_T*TIT*EFF_T*CPR^{-(a_T+1)}\}$$

in which Eqn. 23 has been used to obtain $(\partial MF_T/\partial CPR)$. A similar procedure beginning with Eqn. N.17 is left to the reader. Assumptions used in step 2 different from those given in (16) include: $CPR_C = 11.4$ and $MF_T = 1.15*14.7 = 16.9$ kg/s (37.2 lb/s).

18. For step 3 of the "back-of-the-envelope" calculation, Eqn. N.16 can be differentiated [see (17)] to obtain the change in power output. Since additional heating of the injected fluid is occurring, however, a modified expression for cycle efficiency replaces Eqn. N.17

$$Eff = P/\{MF_C*CP_{comb}*(TIT-T_1-T_1*(CPR^{a_C} - 1)/EFF_C) + (MF_T-MF_C)*CP_{inj}*(30+TIT*EFF_T*(1-CPR^{-a_T}))\} \quad (N.20)$$

in which P is from Eqn. N.16, CP_{inj} is the specific heat of the injected fluid, and 30^oC is the assumed temperature difference between the turbine outlet gas and the added fluid at injection. Equation N.19 can be

differentiated to determine the coefficients in Eqn. 29. The only assumption different from those used in (17) required for this step is that $CP_{inj} = CP_{comb}$.

An auxiliary calculation of the potential heat recovery from the turbine exhaust indicates that there is sufficient energy to heat all of the additional flow to 30°C (54°F) below the turbine exhaust temperature. This auxiliary calculation assumes: gas-side exhaust temperature of the heat recovery device is 147°C (297°F); the "saturation" temperature is 177°C (351°F); and the "enthalpy of vaporization" is 2000 kJ/kg (862 BTU/lb).

19. For the last step of the "back-of-the-envelope" calculation, Eqns. N.16 and N.20 can be differentiated to get the coefficients in Eqns. 33 and 34, using two assumptions different from those in (18): CP_T = 1.5 kJ/kg-K (0.36 BTU/lb-R) and CP_{inj} = 2.0 kJ/kg-K (0.48 BTU/lb-R).

20. The actual STIG-cycle calculation takes account of pressure losses through the combustor and the backpressure that exists at the turbine outlet due to the presence of the duct-burner and HRSG [see (3)].

21. While the superheater outlet temperature difference, ΔT_{so} constrains the peak cycle efficiency as ST/A varies, the ST/A at peak efficiency does not change greatly with changes in ΔT_{so}. Supplementary calculations indicate that from a ΔT_{so} of 60 down to 0°C (108-0°F), the ST/A ratio for peak efficiency increases by about 11%, corresponding to an efficiency increase of about 0.5% and an increase in net power output of about 5%.

The pinch-point temperature difference, ΔT_{pp} is a somewhat more important parameter. When ΔT_{pp} is decreased from 50 to 0°C (90-0°F), the ST/A ratio for peak efficiency increases about 20%. Cycle efficiency increases by about 5% and net power output by about 8%.

22. Most industrial process plants require saturated steam rather than superheated steam. In a STIG system, process steam can be drawn off in the saturated state at the exit of the boiler, while only the steam to be injected passes through the superheater.

23. The FCPs used in the busbar cost calculations at no steam injection and at partial steam injection are based on an assumed stand-alone boiler efficiency of 0.83 and on data from IPT [see (24)]: at no steam injection [i.e., full process-steam load = 9090 kg/hr (20,000 lb/hr) of 1.4 MPa (205 psig) saturated steam], the cycle consumes 13.2 MW (45 MBTU/hr) (LHV) of natural gas and produces 3500 kW of electricity, yielding a FCP of 1.59 kJ/kJ (5422 BTU/kWh) (LHV); at half process steam load, it consumes 14.4 MW (49 MBTU/hr) and produces 4750 kW, for a FCP of 1.59 kWh/kWh (7576 BTU/kWh) (LHV).

24. To calculate the FCP when no-supplemental firing is used, the following assumptions are made: stand-alone boiler efficiency of 83%; 60% condensate return at 93°C (200°F); make-up water at 21°C (70°F); process steam is saturated at 1.2 MPa (175 psia). The International Power Technology Co. (1984) indicates that maximum steam production is 9090 kg/hr (20000 lbs/hr), and fuel consumption (in MBTU/hr, LHV) varies with electrical

output, MW, according to

$$FUEL_{nsf} = 45 + 8*(MW-3.5)/2.5 \qquad (N.21)$$

With the above assumptions, the FCP (with no supplemental firing, expressed in BTU/kWh) is

$$FCP = (1000*FUEL - PSF*21600/BE)/MW \qquad (N.22)$$

where BE is the assumed boiler efficiency, FUEL is expressed in MBTU/hr (LHV) and PSF is the fraction of full process steam produced.

25. All of the assumptions and equations in (24) apply for the calculation of the FCP when supplemental firing is used, except for Eqn. N.22, which is modified to:

$$FUEL_{sf} = FUEL_{nsf} + [25.7*(MW-3.5)/2.5]*\{[PSF-(6-MW)/2.5]/[1-(6-MW)/2.5]\} \qquad (N.23)$$

26. The General Electric LM-5000 unit uses a 2-stage compressor, permitting an intercooler to be incorporated into the system. General Electric claims that since successive stages of the LM-5000 turbine are cooled with compressor bleed air, higher termperatures of the gas at the turbine inlet can be obtained without equally high turbine blade-metal temperatures, if intercooling were used. An electrical generating efficiency of 55% with an output of 108 MW of electricity is claimed to be obtainable with an overall CPR of 33.5, a turbine inlet temperature of 1355°C (2470°F), and a steam-to-air ratio of 0.146 (General Electric, 1984).

Table 1. Typical energy performance indicators for alternative cogeneration systems.

	Fuel fraction converted		Overall First-Law Efficiency	Fuel Chargeable to Power in kJ/kJ (BTU/kWh)(b)	Electricity-to-Steam Ratio in kJ/kJ (kWh/MBTU)	Second Law Efficiency(c)	Fuel Savings Rate (kJ of fuel per kJ to process steam)
	to Elec.	to Steam(a)					
Steam turbine(d)	0.12	0.73	0.85	1.38 (4700)	0.17 (50)	0.40 [0.34]	0.27
Gas turbine(e)	0.30	0.46	0.76	1.60 (5450)	0.64 (188)	0.48 [0.35]	0.86
Combined Cycle(f)	0.35	0.42	0.77	1.49 (5080)	0.84 (245)	0.52 [0.35]	1.21
Diesel(g)	0.35	0.25	0.60	2.02 (6900)	1.38 (405)	0.45 [0.35]	1.01

(a) Saturated steam at 1 MPa (150 psig).
(b) Assuming a stand-alone boiler efficiency of 88%.
(c) Assuming feedwater at 100°C (212°F) and an ambient temperature of 15°C (59°F). Numbers in brackets are second-law efficiencies for separate steam production and electricity generation at a central station power plant.
(d) From Figs. 3.1 and 3.3 in (Nydick, Davis, Dunlay, Fam, Sakhuja, 1976). System capacities were not given in the reference, but the data are probably applicable for systems producing of the order of 50-100 MW of electricity.
(e) From Table 2 in (Kovacik, 1984), for a system producing 73.8 MW of electricity.
(f) From Table 2 in (Kovacik, 1984), for a system producing 87 MW of electricity.
(g) From Figs. 3.1 and 3.3 in (Nydick, Davis, Dunlay, Fam, Sakhuja, 1976). The data are for unjacketed diesels producing of the order of 1-30 MW.

Table 2. Characteristics of the Detroit-Diesel Alison 501-KB(a) turbine-generator set(b).

Compressor	
Pressure Ratio (c)	9.3
Air Flow	14.7 kg/s (32.3 lb/s)
Efficiency (d)	0.833
Turbine	
Peak Continuous Turbine Inlet Temperature	982°C (1800°F)
Efficiency (d)	0.897
Gearbox-Generator Efficiency (e)	0.93
Nominal Peak Electrical Power Output	3500 kW
Dimensions	
Weight	583 kg (1283 lb)
Length	2.3 m (7.6 ft)
Width	0.8 m (2.6 ft)
Height	0.8 m (2.6 ft)

(a) The steam-injected version is the 501-KH.
(b) Unless otherwise indicated, data are from (General Motors, 1983).
(c) From (Leibowitz and Tabb, 1984).
(d) From (Jones, Flynn, and Strother, 1982).
(e) From (Cain, 1985).

Table 3. Estimated capital and incremental operating costs for an Alison 501-KH-based steam-injection cogeneration system (6000 kW(e) peak output).

Fully installed capital cost	$5 million
Includes: Gas-turbine generator HRSG with duct burner Control system Building and miscellaneous Installation	
Incremental operating costs over a steam boiler plant	
Turbine overhaul once every 3 years @	$ 220,000/overhaul
Water consumed during steam-injection operation	$ 2/1000 gallons
Non-turbine maintenance	$ 60,000/year
Additional technical supervision	$ 40,000/year
Insurance	$ 137,500/year
Plant life is estimated to be 20-25 years.	

Source: (Koloseus, 1985)

Table 4. Average 1983 state natural gas prices in $/GJ ($/MBTU), based on LHV.*

1. Hawaii	15.22	(16.05)
2. Maine	8.06	(8.50)
3. Maryland	6.29	(6.64)
4. Connecticut	6.17	(6.51)
5. Montana	5.90	(6.23)
6. New York	5.82	(6.14)
7. Delaware	5.74	(6.05)
8. California	5.60	(5.92)
9. West Virginia	5.50	(5.80)
10. New Hampshire	5.49	(5.79)
11. Rhode Island	5.44	(5.74)
12. Oregon	5.42	(5.72)
13. New Jersey	5.35	(5.65)
14. Pennsylvania	5.35	(5.65)
15. Washington	5.34	(5.63)
16. Vermont	5.33	(5.62)
17. Virginia	5.28	(5.57)
18. Ohio	5.27	(5.56)
19. Idaho	5.05	(5.33)
20. Nevada	5.02	(5.29)
U.S. Average:	4.89	(5.16)

* Natural gas prices are conventionally expressed in terms of higher heating value (HHV), but have been converted in this paper to a lower heating value (LHV) basis, since thermodynamic analyses are typically based on LHV. To convert prices based on LHV to those based on higher heating value, multiply by 0.90, the ratio of LHV to HHV.

Source: (American Gas Association, 1984)

Table 5. Average 1983 state electricity prices in (cents/kWh).

1.	Hawaii	8.94
2.	Alaska	8.41
3.	Rhode Island	7.35
4.	Connecticut	7.09
5.	New Jersey	6.99
6.	Massachusetts	6.88
7.	New Hampshire	6.65
8.	California	6.42
9.	Washington, D.C.	5.72
10.	New Mexico	5.64
11.	Vermont	5.50
12.	Florida	5.27
13.	Michigan	5.23
14.	Pennsylvania	5.23
15.	Illinois	5.22
16.	New York	5.07
17.	Kansas	5.03
18.	Arizona	4.99
19.	Texas	4.95
20.	North Dakota	4.93

Sources: (Edison Electric Institute, 1984)

Table 6. Pacific Gas & Electric (California) rate structure.

Period	May 1 - Sept 30		Oct 1 - Apr 30	
PEAK	12:30pm - 6:30am	M-F	4:30pm - 8:30pm	M-F
MID-PEAK	8:30am - 12:30pm	M-F	8:30am - 4:30pm	M-F
	6:30pm - 10:30pm	M-F	8:30pm - 10:30pm	M-F
	8:30am - 10:30pm	Sa	8:30am - 10:30pm	Sa
OFF-PEAK	10:30pm - 8:30am	Sa	10:30pm - 8:30am	Sa
	All day Sunday and holidays		All day Sunday and holidays	

Electricity Charges	($/kWh) Purchased Electricity (a)	($/kWh) Avoided Cost (b)
PEAK	0.10570	0.08604
MID-PEAK	0.08404	0.08271
OFF-PEAK	0.06396	0.06129
Demand Charge	$1.70/Peak kW per Month	
Firm-Capacity Payment		$60/kW per Year

Natural Gas Price (c) $ 4.95 per MBTU (LHV)

(a) Slightly different rates in each season have been averaged.
(b) As of February 1, 1985.
(c) As of January 1, 1985.

Source: (Pacific Gas & Electric Co., San Francisco, CA, 1985)

Table 7. Annual economic and technical performance scenarios for an example STIG cogeneration facility.

Scenario (a)	IRR (%/yr)	MWh/yr			Annually Averaged Fuel Savings Rate (kJ-fuel/kJ-steam)
		Produced	Consumed	Sold	
A	20	30576	20293	10283	0.51
B	20	37921	20293	17628	0.91
C	21	40621	20293	20328	0.83
D	22	46631	20293	26338	0.66
E	21	52416	20293	32123	0.50

(a) For the plant steam and electricity demand profiles shown in Figure 16a, and

A: Conventional gas-turbine cogeneration with venting of excess exhaust gases at part process-steam load.

B: Steam-injected gas-turbine system with no supplemental firing. Excess electricity available for sale to the grid only during part-load operation.

C: Steam-injected gas-turbine system with supplemental firing to full steam-injection for maximum electricity production during periods when peak avoided cost is paid.

D: Steam-injected gas-turbine system with supplemental firing during periods when peak and mid-peak avoided costs are paid.

E: Steam-injected gas-turbine system with supplemental firing during peak, mid-peak, and off-peak avoided-cost periods.

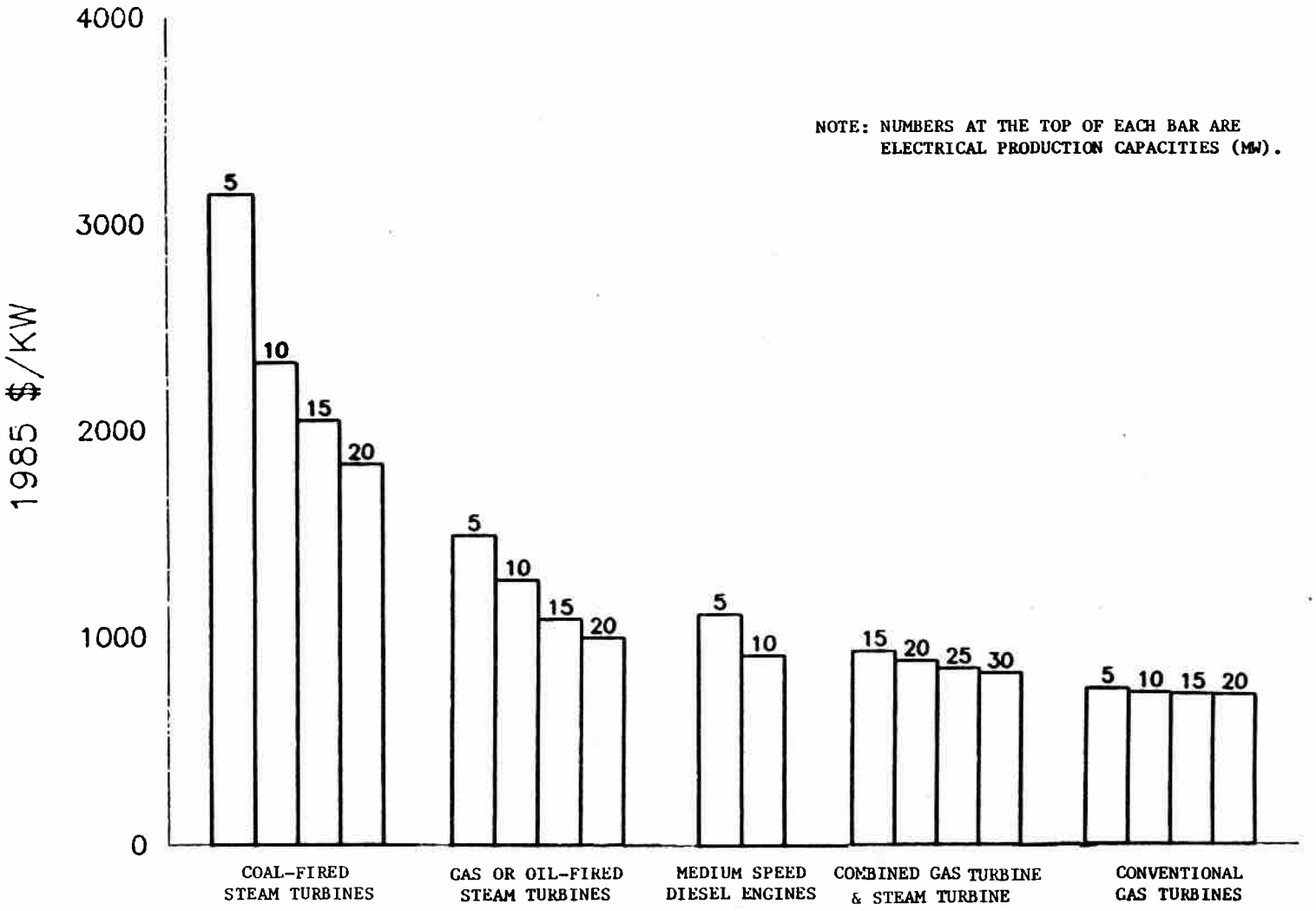

Figure 1. Installed capital costs of small cogeneration systems. Cost data (given in 1980$) are from (Dun & Bradstreet Technical Economic Services, 1984). Costs have been converted to 1985 dollars using the GNP deflator (Council of Economic Advisors, 1985).

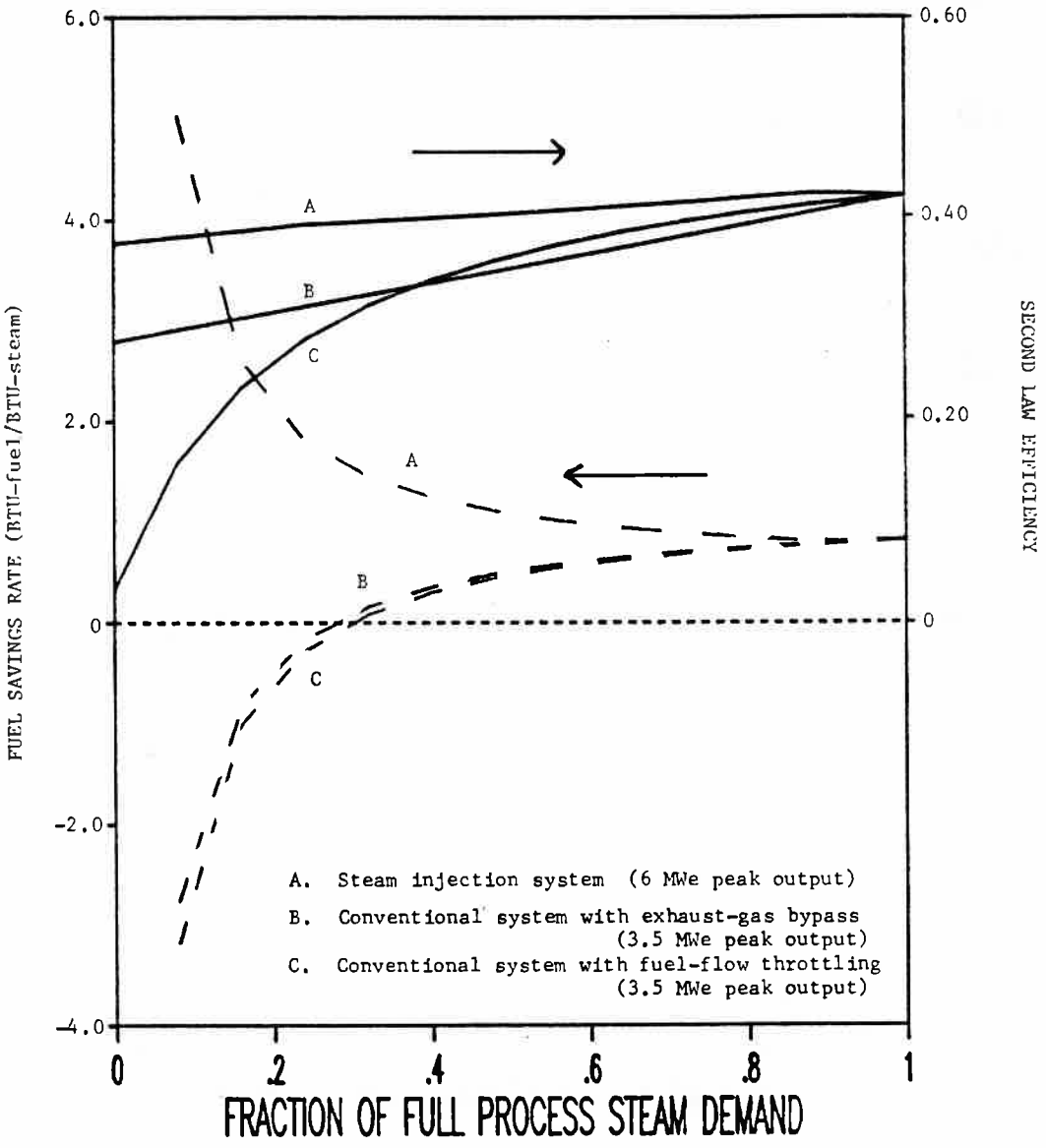

Figure 2. Part-load gas-turbine cogeneration performance: Second-law efficiency and the fuel savings rate (FSR) for two conventional modes of operation and steam-injection operation. The analysis is based on the performance characteristics of systems incorporating the Detroit-Diesel Allison 501-KB or -KH turbine (see Table 2). [Full process-steam demand corresponds to approximately 9100 kg/hr (20,000 lb/hr) of saturated steam at 1 MPa (150 psig).]

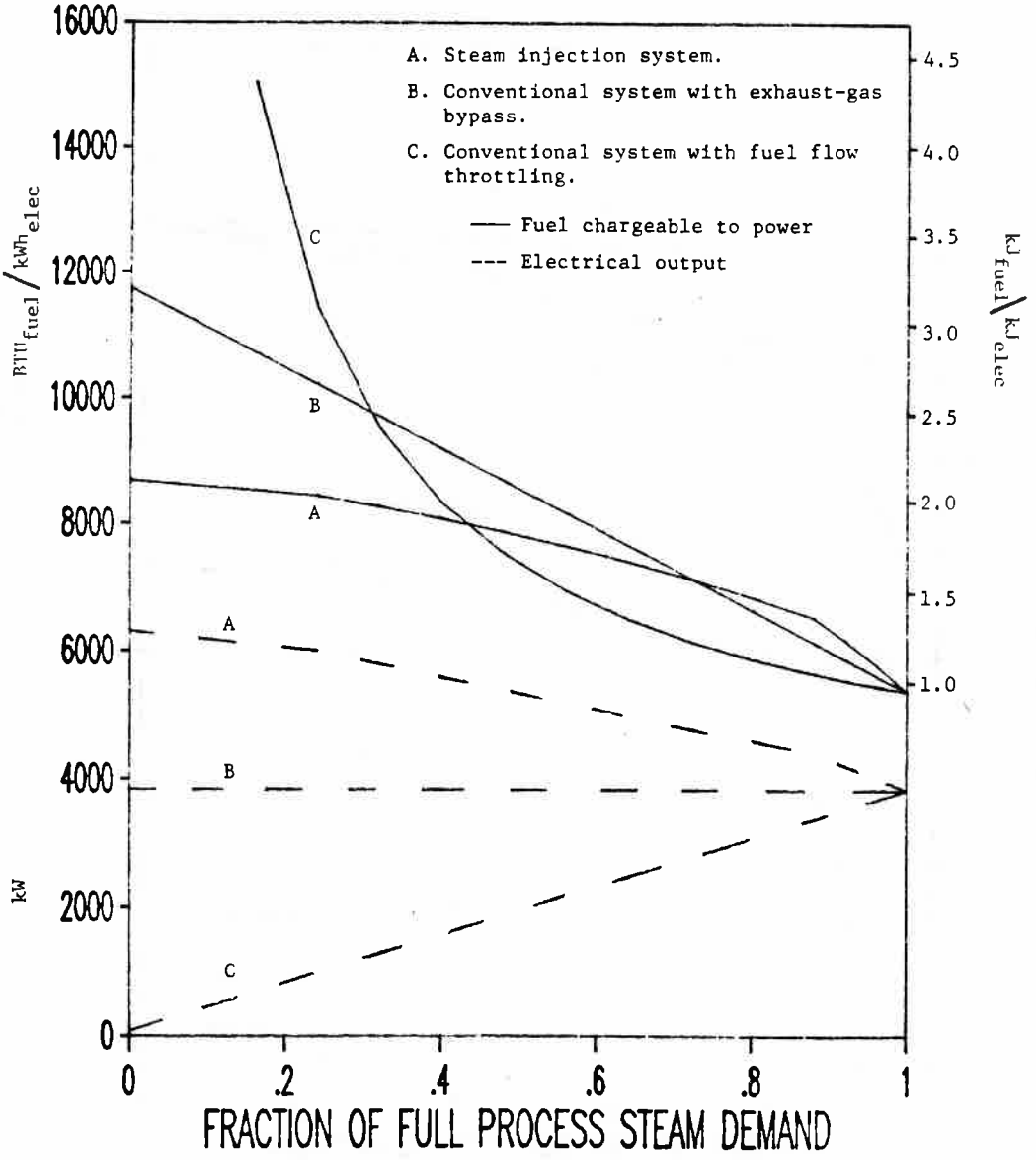

Figure 3. Part-load gas-turbine cogeneration performance: Fuel chargeable to power (FCP) and electricity production (kW) for two conventional modes of operation and steam-injection operation. The analysis is based on the performance characteristics of systems incorporating the Detroit-Diesel Allison 501-KB or -KH turbine (see Table 2). [Full process-steam demand corresponds to approximately 9100 kg/hr (20,000 lb/hr) of saturated steam at 1 MPa (150 psig).]

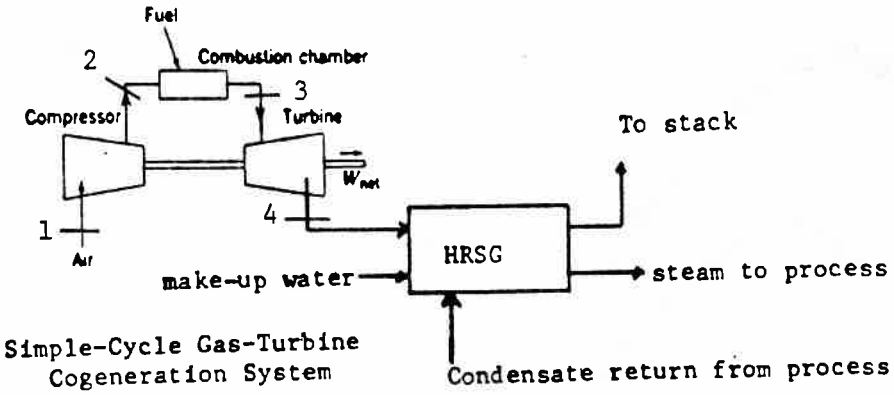

(a)

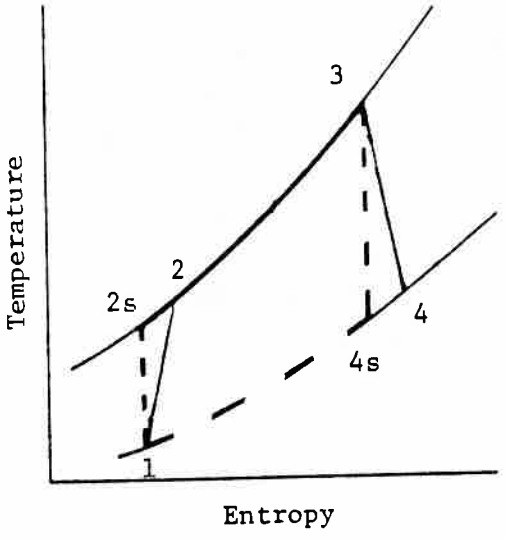

(b)

Figure 4. Schematic (a) and temperature-entropy diagram (b) for a conventional gas-turbine cogeneration cycle.

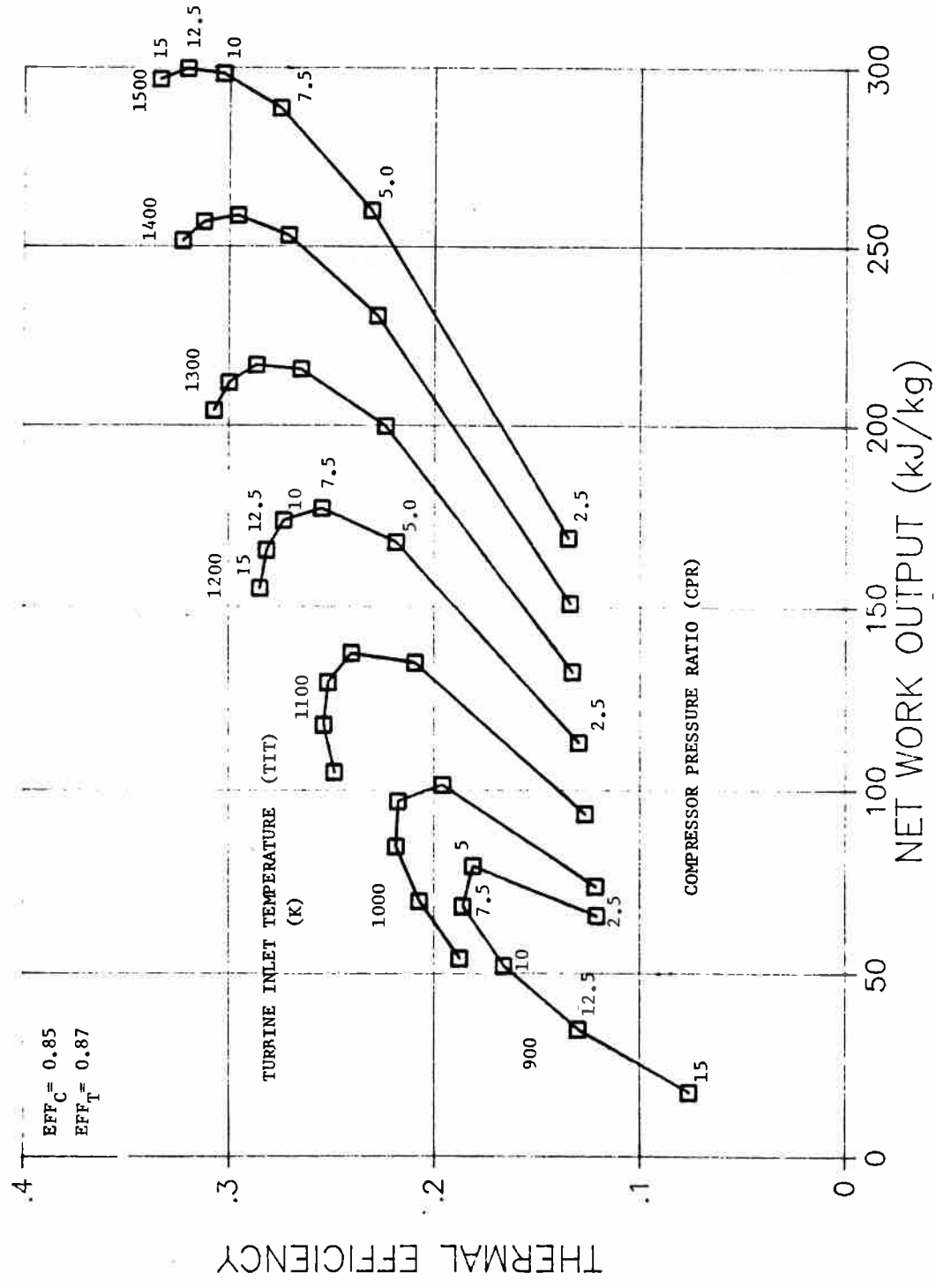

Figure 5. Performance map for a generic simple-cycle gas-turbine power generating system.

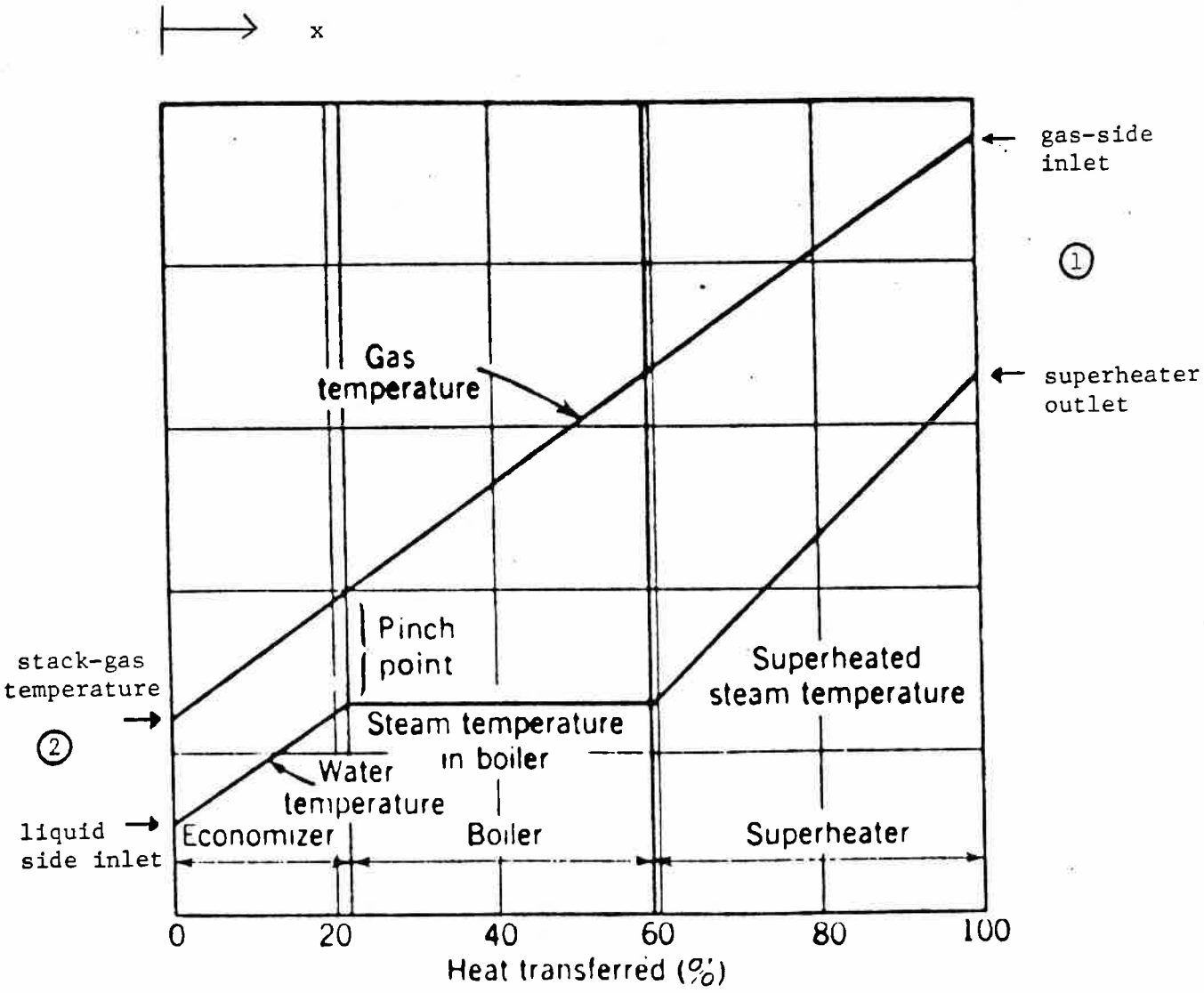

Figure 6. Typcial temperature profiles in a heat recovery steam generator (HRSG).

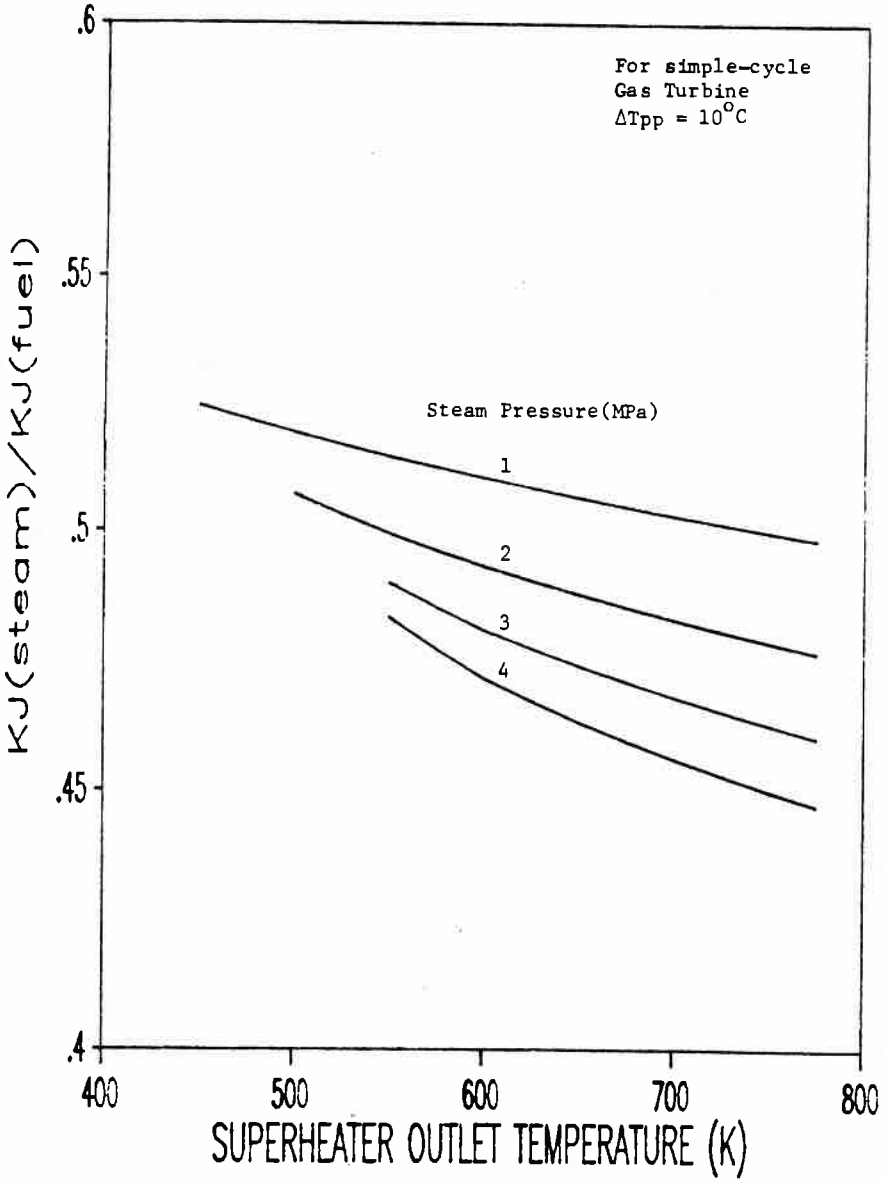

Figure 7. Fraction of gas-turbine fuel converted to steam in the HRSG for a simple-cycle system as a function of steam pressure and superheat. Saturation temperatures are off the left end of each curve. Based on a turbine exhaust temperature of 527°C (981°F) and a pinch point temperature difference of 10°C (18°F).

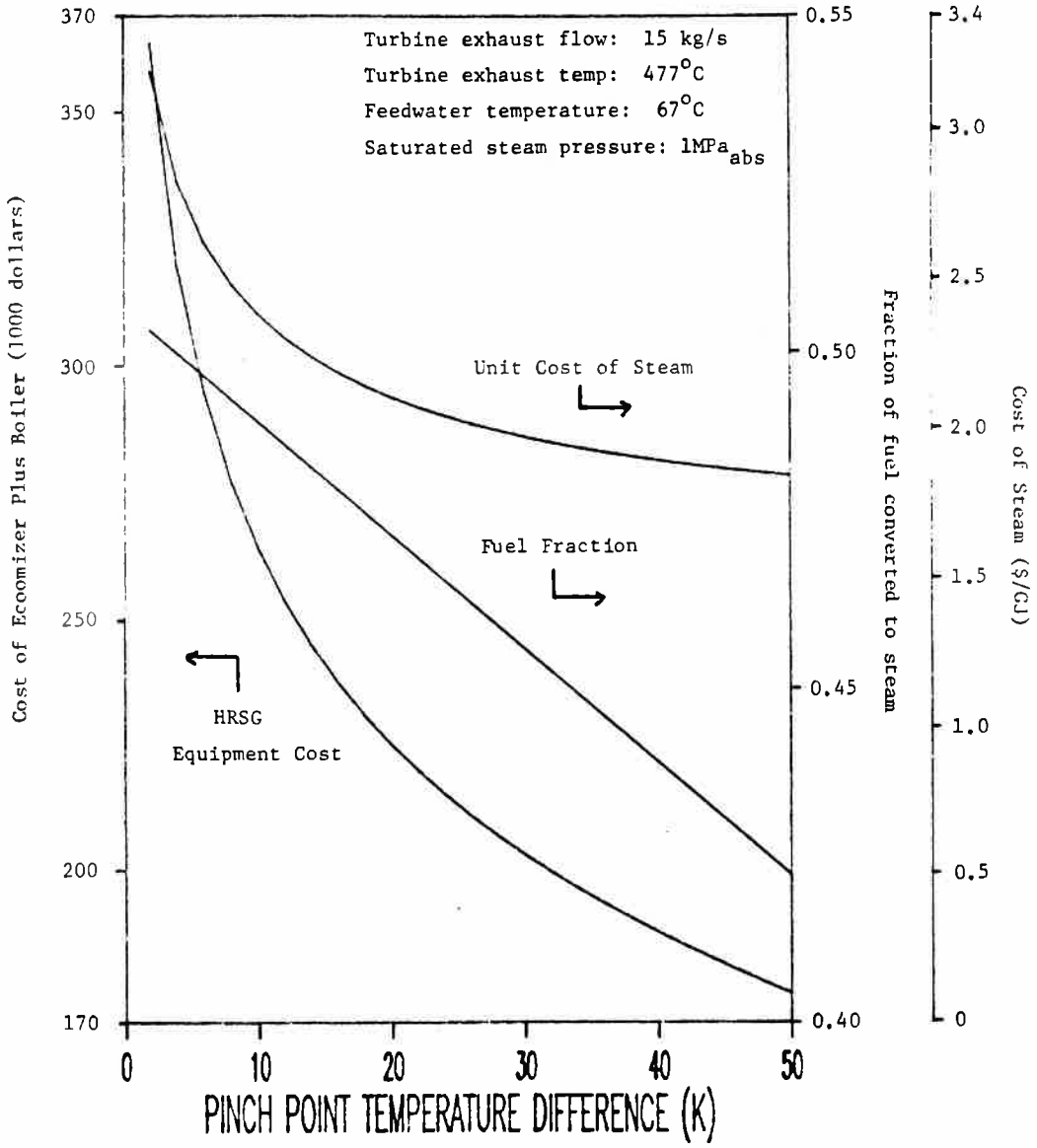

Figure 8. The influence of the pinch point on a simple-cycle gas-turbine cogeneration system. The unit cost of steam represents the capital equipment fraction of the total cost of steam.

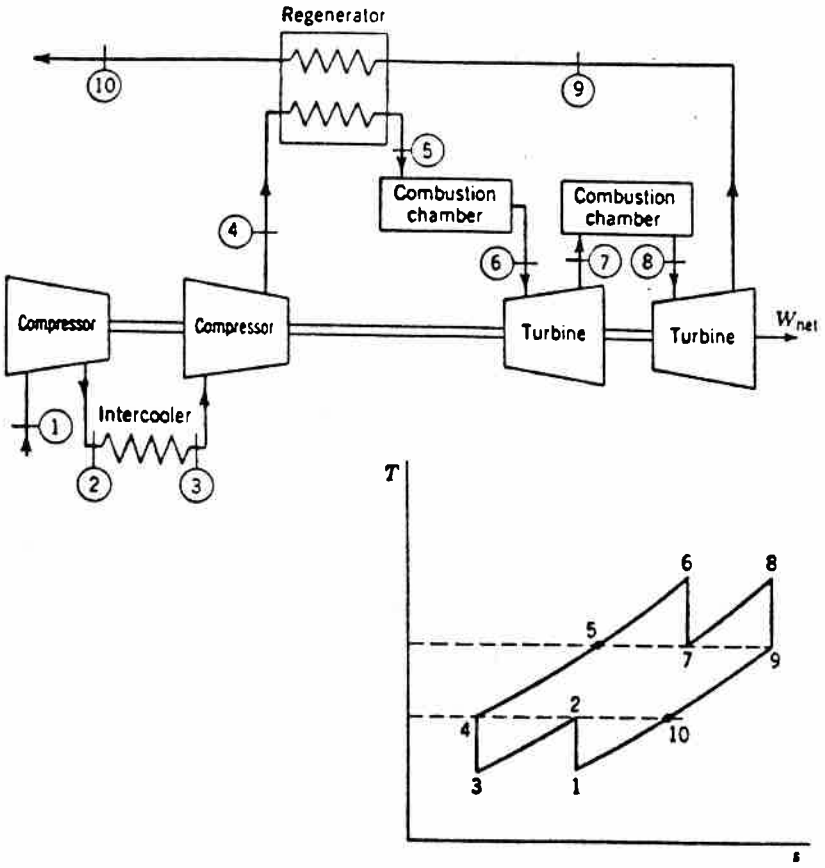

Gas-Turbine Cycle
with Regenerator, Intercooler, and Reheater

Figure 9. Schematic and temperature-entropy diagram for alternative gas-turbine configurations for generating power.

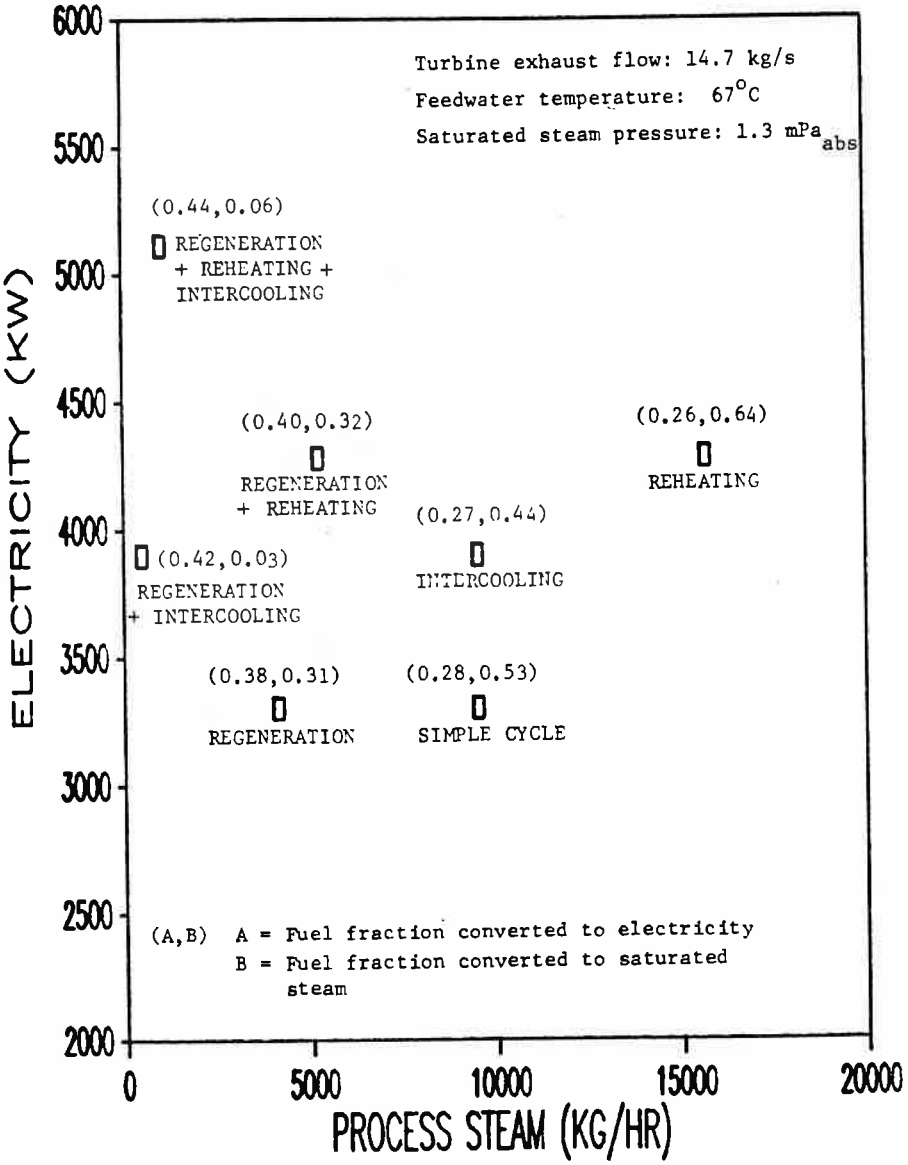

Figure 10. Performance characteristics for alternative simple-cycle gas-turbine cogeneration configurations.

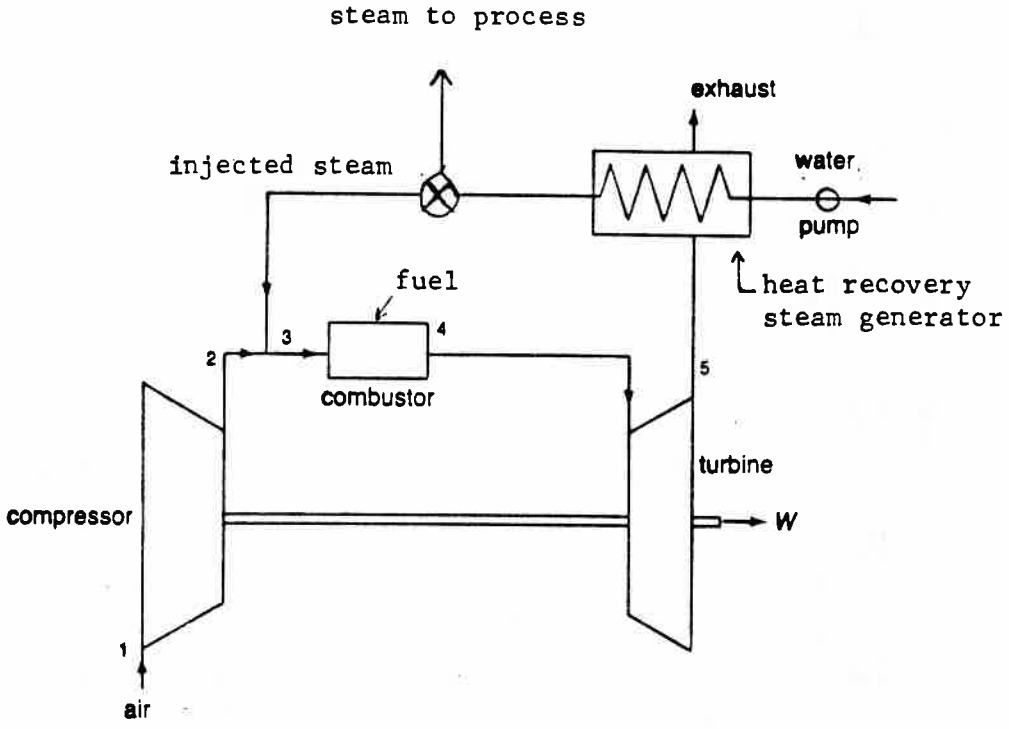

Figure 11. Schematic of a steam-injected gas-turbine cogeneration cycle.

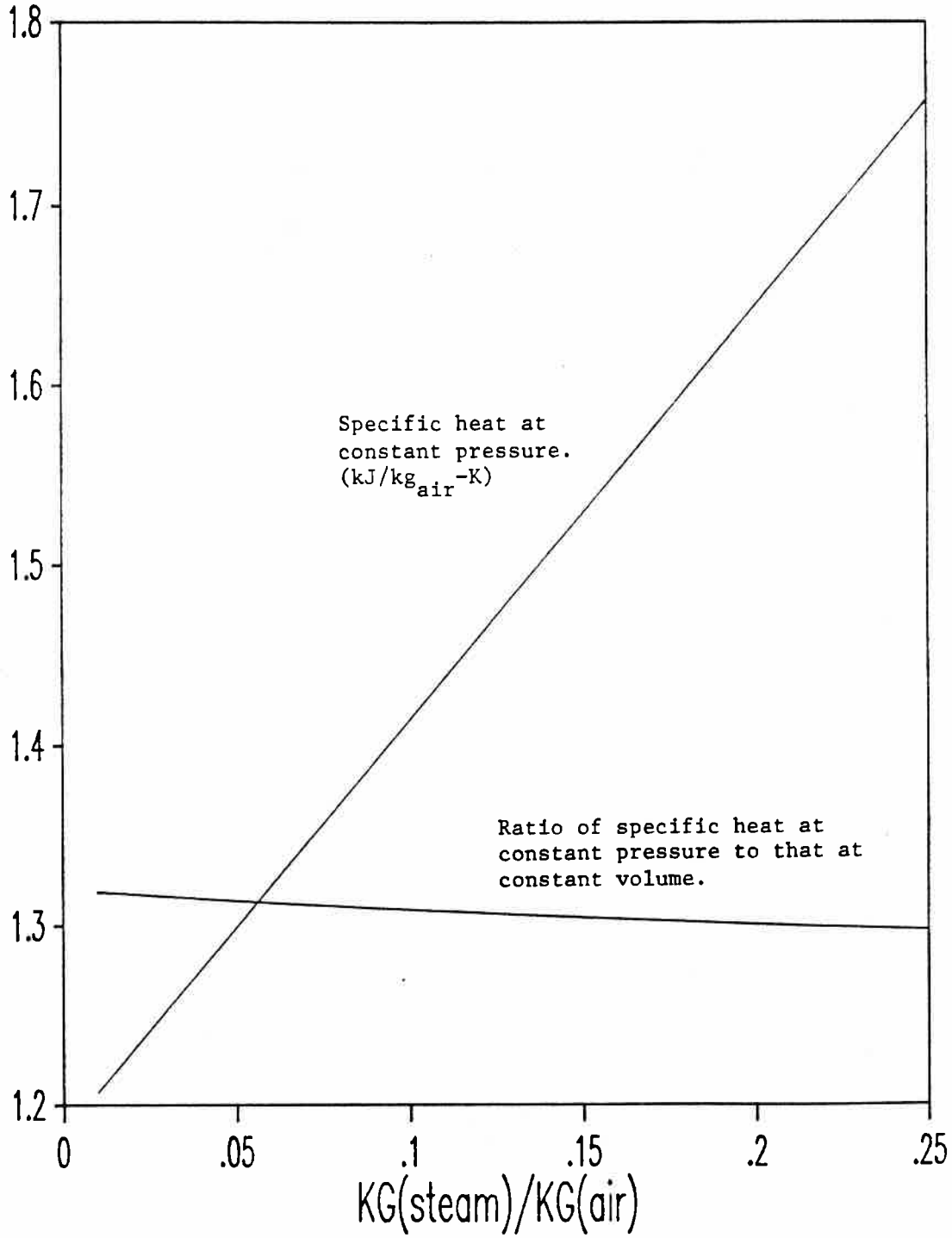

Figure 12. Specific heat parameters for steam-air mixtures at 727°C (1341°F).

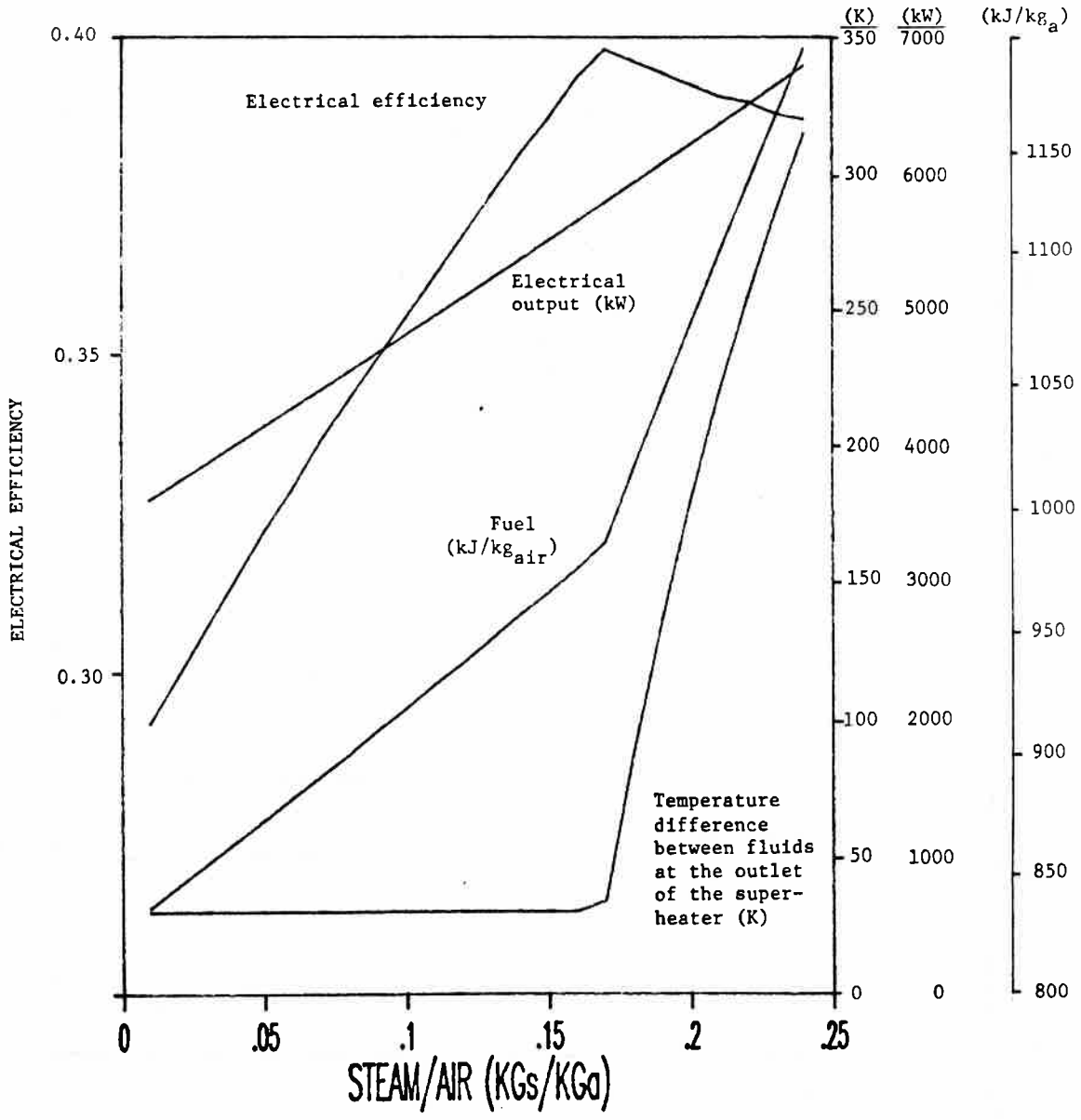

Figure 13. Operating characteristics of a steam-injection cogeneration system based on the Detroit-Diesel Allison 501-KH gas turbine (see Table 2) as a function of the steam-air ratio.

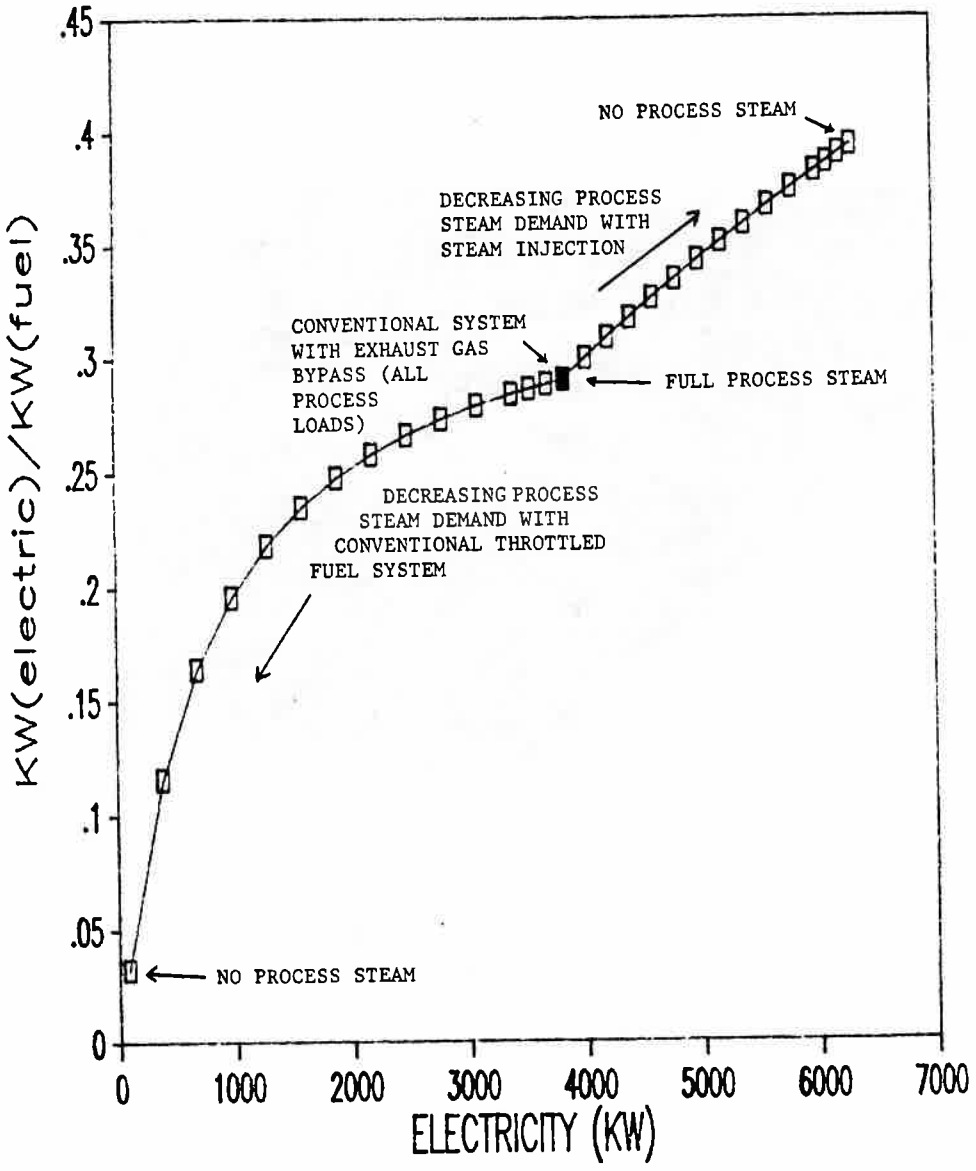

Figure 14. Part-load performance comparison of steam-injected gas-turbine cogeneration and two conventional modes of gas-turbine cogeneration. Analysis based on systems using the Detroit-Diesel Allison 501-KB or -KH turbines (see Table 2).

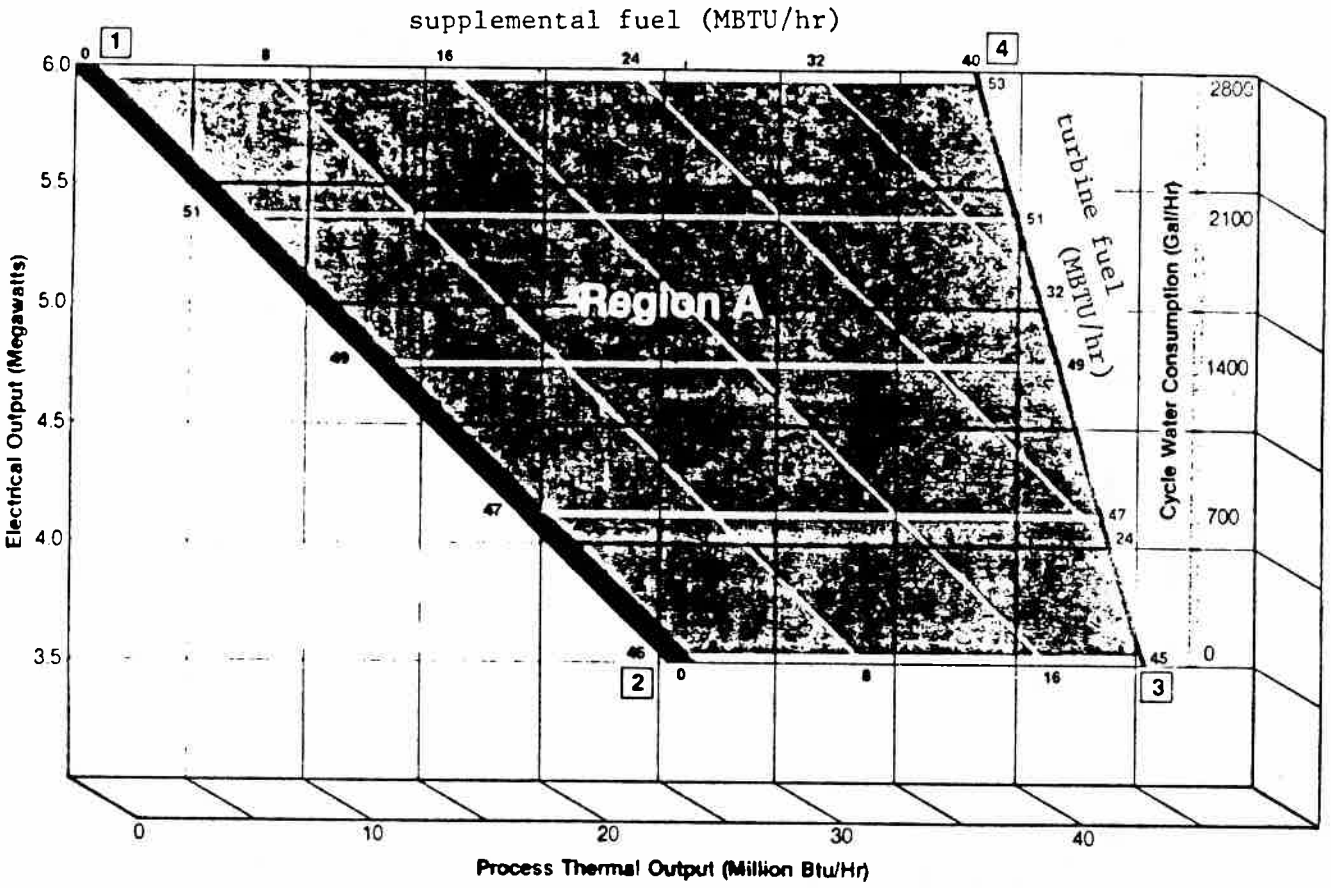

Figure 15. Performance map for a commercial steam-injection cogeneration system with supplemental firing capability. Adapted from (International Power Technology, 1984).

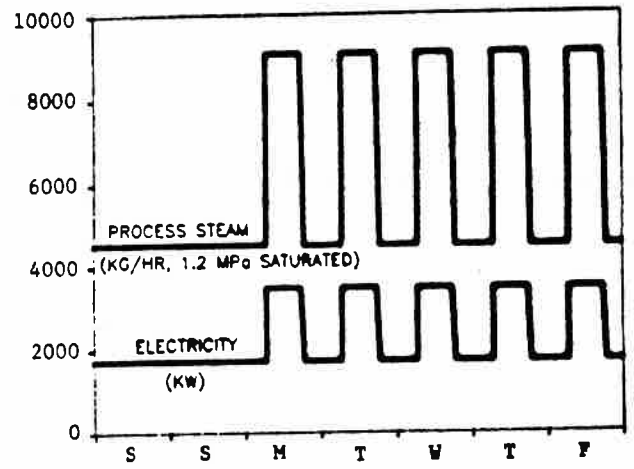

(a) Idealized weekly steam and electricity load profiles for a typical industrial plant.

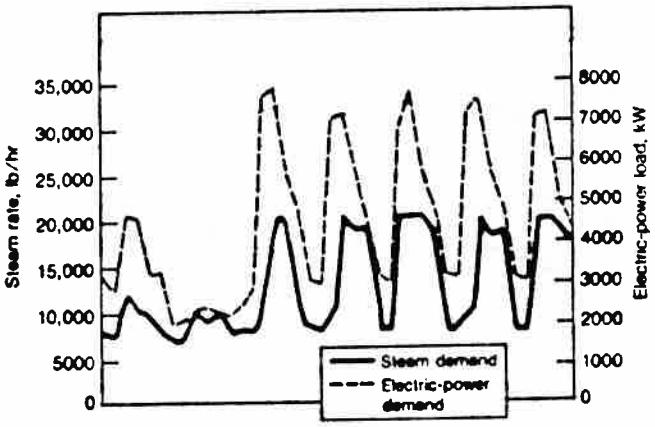

(b) Typical actual weekly steam and electricity profiles for an industrial plant (Kosla, Hamill, and Strothers, 1983).

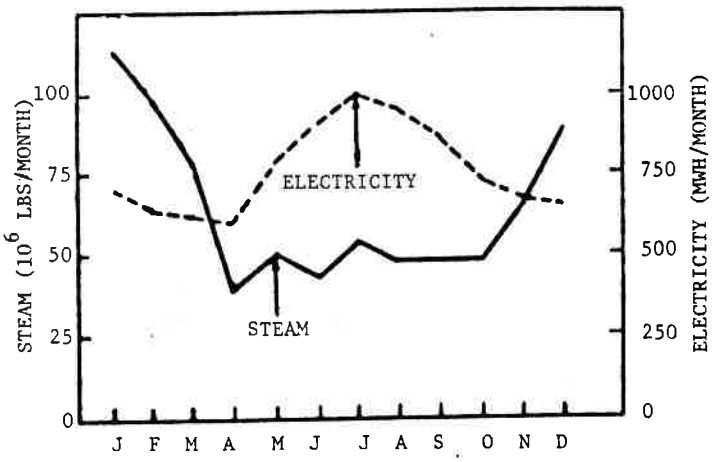

(c) Monthly steam and electricity load profiles for an industrial plant (Pacific Northwest Laboratories, 1984).

Figure 16. Steam and electricity profiles at industrial sites.

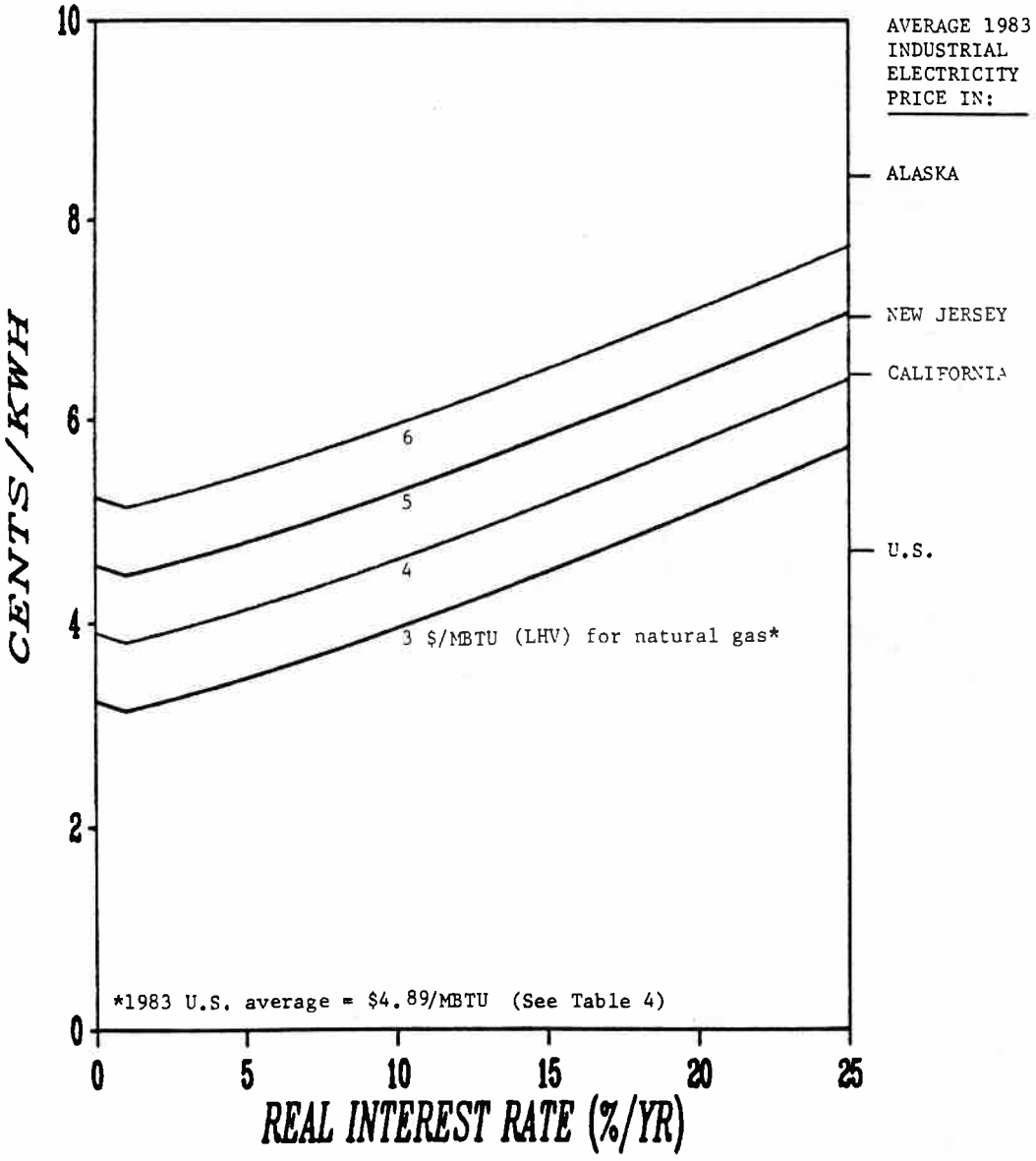

Figure 17. Busbar costs of electricity generated by a steam-injected gas turbine cogeneration system as a function of the real interest rate and for alternative natural gas prices.

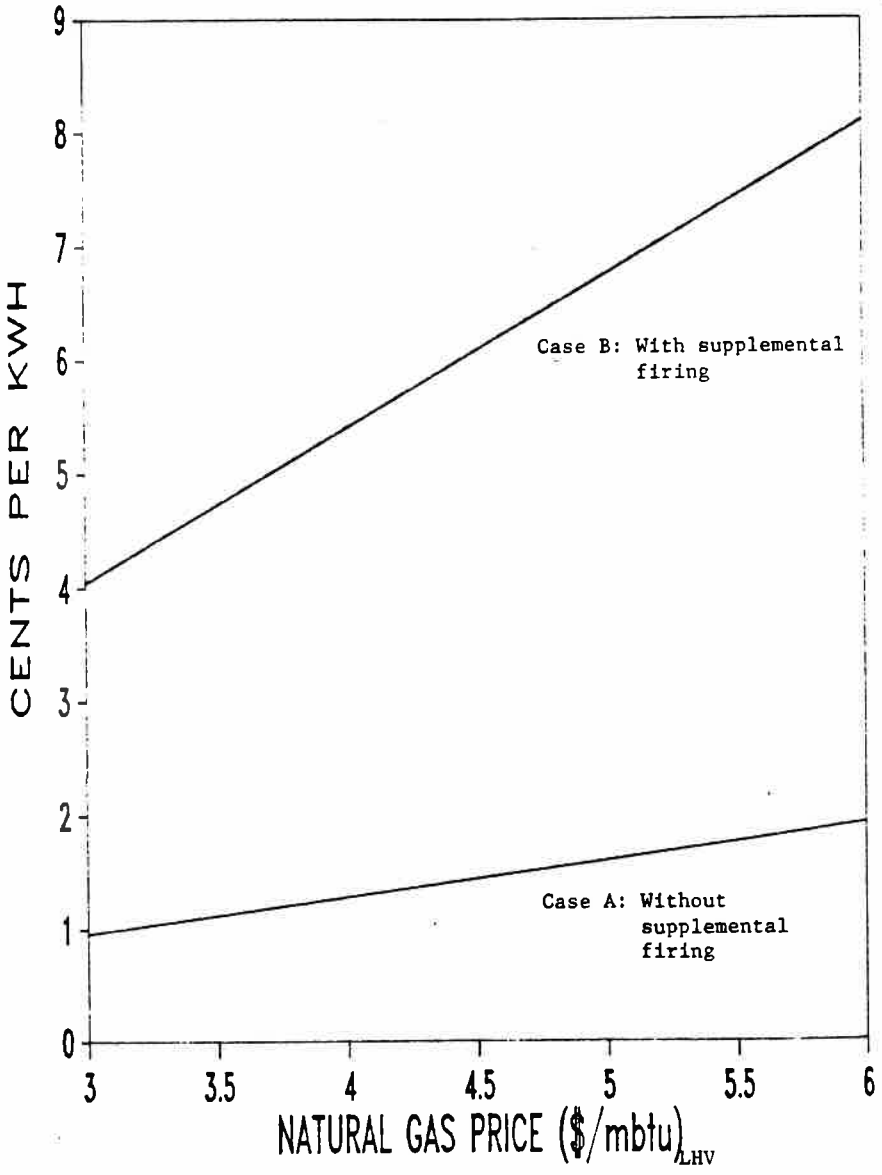

Figure 18. Short-run marginal cost of electricity production for two steam-injected gas-turbine operating modes.

REFERENCES

Abreu, K., Senior Engineer, Pacific Gas and Electric Company, San Francisco, California, personal communication, May 1985.

Allen, R.P. and Kovacik, J.M., "Gas Turbine Cogneration -- Principles and Practice," Journal of Engineering for Gas Turbines and Power (106), October 1984.

American Gas Association, Gas Facts, 1983 Data, AGA, Washington, D.C., 1984.

American Gas Association, "Energy Analysis -- Historical and Projected Natural Gas Prices: 1985 Update," AGA, Arlington, VA, March 15, 1985.

American Institute of Physics, Efficient Use of Energy, AIP Conference Proceedings No. 25, AIP, New York, 1975.

Bechtel Power Corporation, "Coal-Fired Power Plant Capital Cost Estimates," prepared for the Electric Power Research Institute, San Francisco, California, May 1981. Costs given in 1978 dollars were converted to 1984 dollars using the GNP deflators given in (Council of Economic Advisors, 1985).

Bendanillo, V., Energy Coordinator, Sunkist Growers, Inc., Ontario, California, personal communication, April 1985.

Boyce, M.P., Gas Turbine Engineering Handbook, Gulf Publishing Co., Houston, 1982.

Brown, D.H. and Cohn, A., "An Evaluation of Steam Injected Combustion Turbine Systems," Journal of Engineering for Power (103), January 1981.

Cain, G., Mechanical Technology, Inc., Latham, New York, personal communication, April 1985.

Chapman, A.J., Heat Transfer, 3rd Edition, Macmillan, New York, 1974.

Cook, D.S., Design Engineer, Deltak Corporation, Minneapolis, Minnesota, personal communicaton, April 1985.

Council of Economic Advisors, "Economic Indicators," prepared for the Joint Economic Committee, U.S. Government Printing Office, Washington, D.C., April 1985.

Davis, F. and Fraize, W., "Steam-Injected Coal-Fired Gas Turbine Power Cycles," MTR-79W00208, Mitre Corporation, McLean, Virginia, July 1979.

Diamant, R.M.E., Total Energy, Pergamon Press, Oxford, 1970.

Dun & Bradstreet Technical Economic Services and TRW Energy Development Group, "Industrial Cogeneration Potential (1980-2000) for Application of Four Commercially Available Prime Movers at the Plant Site," prepared for U.S. Department of Energy, Office of Industrial Programs, Washington, D.C., August 1984.

Edison Electric Institute, 1983 Statistical Yearbook of the Electric Utility Industry, EEI, Washington, D.C., December 1984.

Electric Power Research Institute, "Technical Assessment Guide," EPRI PS-1201-SR, Palo Alto, California, 1979.

Eriksen, V.L., Froemming, J.M., and Carroll, M.R., "Design of Gas Turbine Exhaust Heat Recovery Boiler Systems," American Society of Mechanical Engineers, paper No. 84-GT-126, New York, 1984.

Fraas, A.P., Engineering Evaluation of Energy Systems, McGraw-Hill, New York, 1982.

Fraize, W.E. and Kinney, C., "Effects of Steam Injection on the Performance of Gas Turbine Power Cycles," Journal of Engineering for Power (101), April 1979.

General Electric Company, "Scoping Study: LM5000 Steam-Injected Gas Turbine," work performed for Pacific Gas and Electric Co., San Francisco, California, July 1984.

General Motors, "Allison Industrial Gas Turbines 501-K, 570-K," company publication, Allison Gas Turbine Operations, General Motors company, Indianapolis, Indiana, 1983.

Haywood, R.W., Analysis of Engineering Cycles, 3rd Edition, Pergamon Press, Oxford, 1980.

International Power Technology, "Cheng Cycle Series 7-Cogen," company publication, Palo Alto, California, received March 1984.

Jones, J.L., Program Manager, International Power Technology, Inc., Palo Alto, California, personal communication, April 1985.

Jones, J.L., Flynn, B.R., and Strother, J.R., "Operating Flexibility and Economic Benefits of a Dual-Fluid Cycle 501-KB Gas Turbine Engine in Cogeneration Applications," American Society of Mechanical Engineers, paper No. 82-GT-298, New York, 1984.

Koloseus, C., Director of Market Development, International Power Technology, Inc., Palo Alto, California, personal communication, April 1985.

Kosla, L., Hamill, J., and Strothers, J., "Inject steam in a gas turbine -- but not just for NO_x control," Power, February 1983.

Kovacik, J.M., "Cogeneration Application Considerations," Gas Turbine Reference Library, GER-3430, General Electric Company, Schenectady, New York, 1984.

Leibowitz, H., Mechanical Technology, Inc., Latham, New York, personal communication, May 1985.

Leibowitz, H. and Tabb, E., "The Integrated Approach to a Gas Turbine Topping Cycle Cogeneration System," Journal of Engineering for Gas Turbines and Power (106), October 1984.

Lovell, B., Design Engineer, Deltak Corporation, Minneapolis, Minnesota, personal communication, May 1985.

Mark's Handbook for Mechanical Engineers, 8th edition, Baumeister and Marks (eds.), McGraw-Hill, New York, 1978.

Maslennikov, V. and Shterenberg, V.Y., "Power Generating Steam Turbine-Gas Turbine Plant for Covering Peak Loads," Thermal Engineering 21(4), 1974.

Nydick, S.E., Davis, J.P., Dunlay, J., Fam, S., Sakhuja, R., "A Study of Inplant Electric Power Generation in the Chemical, Petroleum Refining, and Paper and Pulp Industries," prepared for the Federal Energy Administration by Thermo Electron Corp., Waltham, Mass., 1976.

Pacific Gas and Electric Company, company rate schedules, San Francisco, California, January 1985.

Pacific Northwest Laboratories, "Cogeneration Handbook for the Food Processing Industry," US Department of Energy, DOE/NBB-0061, Washington, D.C., February 1984.

Price, D., Senior Engineer, Pacific Gas and Electric Company, San Francisco, California, personal communication, May 1985.

Sonntag, R.E. and Van Wylen, G., Introduction to Thermodynamics, 2nd Edition, Wiley, New York, 1982.

Wark, K. Thermodynamics, 3rd Edition, McGraw-Hill, New York, 1977.

Williams, R.H., "Industrial Cogeneration," The Annual Review of Energy (3), 1978.

Wilson, W.B., "Gas Turbine Cycle Flexibility for the Process Industry," GER-2229M, General Electric Company, Schenectady, New York, 1978.